

2015

Analysis and performance evaluation of SISO and MIMO OFDM channel estimation techniques using pilot symbols

Imtiyaz Ahmed Mohammed

Follow this and additional works at: <https://huskiecommons.lib.niu.edu/allgraduate-thesesdissertations>

Recommended Citation

Mohammed, Imtiyaz Ahmed, "Analysis and performance evaluation of SISO and MIMO OFDM channel estimation techniques using pilot symbols" (2015). *Graduate Research Theses & Dissertations*. 1435. <https://huskiecommons.lib.niu.edu/allgraduate-thesesdissertations/1435>

This Dissertation/Thesis is brought to you for free and open access by the Graduate Research & Artistry at Huskie Commons. It has been accepted for inclusion in Graduate Research Theses & Dissertations by an authorized administrator of Huskie Commons. For more information, please contact jschumacher@niu.edu.

ABSTRACT

ANALYSIS AND PERFORMANCE EVALUATION OF SISO AND MIMO OFDM CHANNEL ESTIMATION TECHNIQUES USING PILOT SYMBOLS

Imtiyaz Ahmed Mohammed, M.S.
Department of Electrical Engineering
Northern Illinois University, 2015
Mansour Tahernezehadi, Thesis Director

Multiple input multiple output orthogonal frequency division multiplexing (MIMO OFDM) provides a significant performance gain compared to the single antenna systems by using diversity and multiplexing techniques. The availability of channel state information at the receiver determines the multiplexing and diversity gain of the MIMO OFDM systems. In this thesis work, analysis and comparison of different pilot-aided channel estimation algorithms have been performed. The Alamouti space frequency block coding (SFBC) is used to achieve diversity, whereas maximum likelihood (ML) detector is used to decode the spatially coded symbols.

The pilot-aided channel estimation is performed for both MIMO and single input single output (SISO) OFDM systems using the least square (LS) and minimum mean square error (MMSE) channel estimation algorithms for the block-type and comb-type pilots. MATLAB simulations have been performed for estimating the channel in different scenarios like Rayleigh fading and Stanford university interim (SUI) channel models at various Doppler frequencies. The performance of different channel estimators have been evaluated for a 2x2 and 1x1 system using the mean square error (MSE) and bit error rate (BER). The MMSE estimator performs better than LS estimator in terms of BER but is a little complex. At low Doppler frequencies MMSE

estimator using block-type pilots performs better while at high Doppler frequencies MMSE estimator using comb-type pilots performs better. The SUI channel model performed better than the Rayleigh channel due to presence of line of sight (LOS). Hence, the comb type MMSE estimator in MIMO OFDM is optimal in fast fading scenarios.

NORTHERN ILLINOIS UNIVERSITY

DEKALB, ILLINOIS

MAY 2015

ANALYSIS AND PERFORMANCE EVALUATION OF SISO AND MIMO
OFDM CHANNEL ESTIMATION TECHNIQUES USING PILOT SYMBOLS

BY

IMTIYAZ AHMED MOHAMMED

©2015 Imtiyaz Ahmed Mohammed

A THESIS SUBMITTED TO THE GRADUATE SCHOOL
IN PARTIAL FULFILLMENT OF THE REQUIREMENTS

FOR THE DEGREE

MASTER OF SCIENCE

DEPARTMENT OF ELECTRICAL ENGINEERING

Thesis Director:
Mansour Tahernezehadi

ACKNOWLEDGEMENTS

I would like to take this opportunity to sincerely thank my advisor, Dr. Mansour Tahernezehadi, for his consistent motivation, guidance, and valuable advice during my master's program. It helped me a lot in understanding and solving the problems faced during this thesis work. It has been a learning and wonderful experience in my life to be a Master of Science student in the Department of Electrical Engineering at Northern Illinois University, Illinois.

I would like to thank Dr. Donald Zinger and Dr. Peng Yung Woo, members of my thesis committee, for their valuable suggestions and precious time.

I would like to thank my parents for their unconditional love, support and faith in me. Also, I would like to express gratitude to friends for their constant support and useful advice.

TABLE OF CONTENTS

	Page
LIST OF TABLES.....	v
LIST OF FIGURES.....	vi
CHAPTER 1: INTRODUCTION.....	1
1.1 Background.....	1
1.2 Problem Statement.....	2
1.3 Thesis Organization.....	4
CHAPTER 2: WIRELESS CHANNELS AND THEIR CHARACTERISTICS	5
2.1 Wireless Channels.....	5
2.2 Large-Scale Fading.....	6
2.3 Small-Scale Fading.....	6
2.3.1 Multipath Effect.....	6
2.3.2 Coherence Bandwidth.....	7
2.3.3 Doppler Effect.....	7
2.3.4 Coherence Time.....	8
2.4 Doppler Spectrum.....	8
2.5 Rayleigh Fading.....	9
2.6 Ricean Fading.....	9
2.7 SUI Channels.....	10
CHAPTER 3: OFDM AND MIMO OFDM	11
3.1 Introduction.....	11
3.1.1 Transmitter Schematic.....	11
3.1.2 Receiver Schematic.....	12

	Page
3.1.3 Cyclic Prefix	13
3.2 OFDM Merits	14
3.3 OFDM Demerits	15
3.4 MIMO OFDM.....	15
3.4.1 Spatial Diversity.....	16
3.4.2 Transmit Diversity	16
3.4.3 Receive Diversity.....	17
3.4.4 Spatial Multiplexing.....	17
3.4.5 Beam Forming	18
3.5 Alamouti STBC	18
3.6 Alamouti SFBC.....	19
3.7 Maximum Likelihood Detector.....	21
CHAPTER 4: CHANNEL ESTIMATION FOR SISO AND MIMO OFDM SYSTEMS	23
4.1 Introduction.....	23
4.2 Block-Type Pilots	23
4.3 Comb-Type Pilots	24
4.3.1 Interpolation Techniques.....	25
4.4 SISO OFDM Channel Estimation.....	26
4.4.1 Using Block-Type Pilots.....	27
4.4.2 Using Comb-Type Pilots.....	29
4.5 MIMO OFDM Channel Estimation	30
4.5.1 Using Block-Type Pilots.....	32
4.5.2 Using Comb-Type Pilots.....	32
CHAPTER 5: SIMULATION RESULTS AND COMPARISON.....	34
5.1 MSE Comparison for a Rayleigh Channel.....	34
5.2 BER Comparison for a Rayleigh Channel	38

	Page
5.3 MSE Comparison for a SUI-3 Channel	41
5.4 BER Comparison for a SUI-3 Channel.....	45
5.5 BER vs Normalized Doppler Comparison for a Rayleigh Channel.....	48
5.6 BER vs Normalized Doppler Comparison for a SUI-3 Channel	49
CHAPTER 6: CONCLUSION AND FUTURE WORK	51
6.1 Conclusion	51
6.2 Future Work.....	52
REFERENCES	53

LIST OF TABLES

	Page
Table 2. 1 SUI channel terrain type, Doppler and delay spreads [9]	35
Table 5.1 Simulation parameters for a Rayleigh channel	35
Table 5.2 SUI-3 channel parameters.....	41
Table 5.3 Simulation parameters for a SUI-3 channel.....	42

LIST OF FIGURES

	Page
Figure 2.1: Representation of distance between MS and BS	5
Figure 2.2: MS and BS angle representation	8
Figure 3.1: Transmitter schematic of an OFDM system.....	12
Figure 3.2: Receiver schematic of an OFDM system	13
Figure 3.3: Cyclic prefix insertion	14
Figure 3.4: MIMO system.....	16
Figure 3.5: Block diagram of transmit diversity	17
Figure 3.6: Block diagram of receive diversity.....	17
Figure 4.1: Block-type pilot arrangement [1]	24
Figure 4.2: Comb-type pilot arrangement [1]	25
Figure 4.3: Block diagram of SISO OFDM channel estimation.....	26
Figure 4.4: MMSE channel estimation overview	29
Figure 4.5: Block diagram of MIMO OFDM channel estimation	31
Figure 5.1 MSE vs SNR plot in a Rayleigh channel at normalized Doppler of 0.0008.....	36
Figure 5.2 MSE vs SNR plot in a Rayleigh channel at normalized Doppler of 0.024.....	37
Figure 5.3 MSE vs SNR plot in a Rayleigh channel at normalized Doppler of 0.048.....	38
Figure 5.4 BER vs SNR plot in a Rayleigh channel at normalized Doppler of 0.0008	39
Figure 5.5 BER vs SNR plot in a Rayleigh channel at normalized Doppler of 0.024	40
Figure 5.6 BER vs SNR plot in a Rayleigh channel at normalized Doppler of 0.048	41
Figure 5.7 MSE vs SNR plot in a SUI-3 channel at normalized Doppler of 0.0008	43

Figure 5.8 MSE vs SNR plot in a SUI-3 channel at normalized Doppler of 0.024	44
Figure 5.9 MSE vs SNR plot in a SUI-3 channel at normalized Doppler of 0.048	45
Figure 5.10 BER vs SNR plot in a SUI-3 channel at normalized Doppler of 0.0008.....	46
Figure 5.11 BER vs SNR plot in a SUI-3 channel at normalized Doppler of 0.024.....	47
Figure 5.12 BER vs SNR plot in a SUI-3 channel at normalized Doppler of 0.048.....	48
Figure 5.13 BER vs normalized Doppler plot for Rayleigh channel at SNR=12db	49
Figure 5.14 BER vs normalized Doppler plot for SUI-3 channel at SNR=12db	50

CHAPTER 1: INTRODUCTION

1.1 Background

Wireless communications have brought about a revolution in the field of communications. In recent years, with the rapid growth of mobile communication services and emerging broadband mobile Internet access services the optimization of wireless communication system has become critical [1]. The development of high-performance and bandwidth-efficient wireless transmission technology is dependent on the estimation of wireless channels and its characteristics.

OFDM is a multicarrier modulation scheme which is the basis for modern wireless communication standards. OFDM modulation has been adopted as a physical layer scheme for many modern broadband wireless air interface standards, such as fourth-generation (4G) Long Term Evolution (LTE), IEEE 802.11/Wi-Fi (Wireless Fidelity), IEEE 802.16/WiMAX (Worldwide Interoperability for Microwave Access), as well as Digital Video Broadcast – Terrestrial (DVB-T) [2]. In an OFDM system, at the transmitter the information bit sequence is modulated into PSK/QAM symbols, then the IFFT is performed on the symbols so that they are converted into time-domain signals and transmitted through a wireless channel. The signal received at the receiver is usually distorted due to the channel characteristics.

To recover the transmitted bits, the effect of the wireless channel must be estimated and compensated at the receiver. As long as there is no ICI (inter-carrier interference), the orthogonality among the subcarriers is preserved and each subcarrier can be considered as an independent channel. The received signal can be expressed as the product of transmitted signal and channel frequency response at the subcarrier. Thus, by estimating the channel frequency

response the transmitted signal can be recovered at each subcarrier. The channel estimation is of great importance in coherent demodulation schemes and affects the system's performance. MIMO OFDM is one of the latest techniques to increase the performance of the wireless communication system by using multiple antennas both at the transmitter and receiver. MIMO techniques can be used to increase diversity, data rate by spatial multiplexing and beam forming. As multiple antennas are used, the system becomes complex and channel estimation is not easy as compared to SISO OFDM.

1.2 Problem Statement

As the channel estimation is necessary for coherent demodulation schemes, it has to be estimated accurately in order for the system to perform better. The channel estimation can be broadly divided into two types. One is the blind channel estimation which exploits the statistical characteristics of the channel and certain properties of the transmitted signals. The other is called pilot symbol-aided or training-based channel estimation, which uses the pilot symbols known to both transmitter and receiver to estimate channel at the pilot frequencies and employs various interpolation schemes to estimate the channel at data subcarriers. Though the blind channel estimation has an advantage that it has no overhead loss, it's only applicable in slowly time-varying channels because it requires a long data record. Different factors are usually considered for channel estimation of any OFDM system like the feasibility of implementation, performance requirements, complexity and rapid changes in the fast-varying channel. In this thesis for estimating the time-varying wireless channels we use the pilot symbols which are known at the receiver in advance to get accurate information about the channel.

The pilot symbols scheme can be used to send pilots either in time domain at different OFDM symbols or in frequency domain at different subcarriers. In pilot symbol-aided channel estimation two important things to consider are design of pilots and interpolation [3]. The time-domain way of sending the pilots is known as block-type pilot symbols and the frequency-domain way is known as comb-type pilot symbols. The block-type method is used in slowly time-varying channels, whereas the comb-type method is used in fast time-varying channels where channel changes from one OFDM symbol to another. MIMO OFDM is one of the important and widely used techniques in modern wireless communications. The capacity as well as diversity of communication systems can be increased by using multiple antennas at the transmitter and receiver. Moreover the multiple antennas do not use any additional power. But the capacity and diversity improvement comes at the cost of system complexity. As multiple antennas are used both at the transmitter and receiver, estimation of channel state information becomes complex.

Many techniques have been proposed related to the channel estimation [4-6]. But most of the techniques increase the amount of calculations and thus increase the complexity. In Mata et al [6], space time block coding is used as MIMO technique but the channel is assumed to be constant for two consecutive symbols, which is not the case in fast time-varying channels. In this work SFBC is used as MIMO technique in which symbols are transmitted at adjacent subcarriers in an OFDM symbol and orthogonal pilots are used for channel estimation. In orthogonal pilot scheme the pilots are transmitted in such a way that when one antenna transmits a pilot, the other antenna remains silent or does not transmit anything. In Wang Liping [5], a least square-based channel estimation method using orthogonal pilots has been proposed. By using orthogonal pilots the channel estimation becomes simple and similar to SISO OFDM channel estimation as

at one frequency instant only one antenna transmits the pilot symbols. Once the channel coefficients are estimated then the received symbols can be estimated by using the maximum likelihood detection algorithm.

1.3 Thesis Organization

This thesis work is organized as follows:

- In Chapter 2, various wireless channel models and its characteristics are explained. The important factors like the coherence bandwidth and coherence time of a channel are thoroughly explained.
- In Chapter 3, the basics of SISO OFDM and MIMO OFDM systems are explained in detail. Various MIMO techniques like STBC and SFBC are discussed.
- Chapter 4 contains various channel estimation techniques like LS and MMSE for SISO and MIMO OFDM systems. Different pilot patterns along with various channel estimation algorithms are thoroughly explained.
- Chapter 5 contains the parameters used in simulations and results of channel estimation techniques mentioned in this thesis.
- In Chapter 6 conclusions of the thesis along with the future research scope are suggested.

CHAPTER 2: WIRELESS CHANNELS AND THEIR CHARACTERISTICS

2.1 Wireless Channels

In wireless channels, the signal strength decreases as the distance of propagation increases. Let 'd' be the distance between base station (BS) and mobile station (MS) as seen from Figure 2.1. Then signal strength at the MS can be characterized as a function of 'd'. Hence there is a need for models which predict the mean signal strength at the receiver as a function of separation between transmitter and receiver. These models are termed large-scale propagation models. Free space propagation model predicts the received signal strength when there is an unobstructed propagation path between the transmitter and receiver. The Frii's free space equation is given by [1]:

$$P_r(d) = \frac{P_t G_t G_r \lambda^2}{(4\pi)^2 d^2 L} \quad (2.1)$$

where P_r is the received power as a function of 'd', P_t is the transmitted power, L is the system loss factor, λ is wavelength, G_t is transmit antenna gain and G_r is receiver antenna gain.

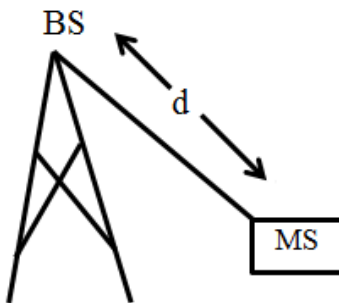


Figure 2.1: Representation of distance between MS and BS.

Due to some atmospheric effects like scattering, reflection and diffraction, the signal undergoes a change in its amplitude and phase. The variation in signal amplitude with respect to time and frequency is called fading. Fading occurs due to multipath propagation or reflection from obstacles which change the direction of propagation of a signal. Fading can be broadly classified into two types: large-scale fading and small-scale fading.

2.2 Large-Scale Fading

The fading that arises when base station and mobile terminal are separated by a large distance is known as large scale fading. It is caused by reflection from buildings, hilly terrains and various obstacles. It is determined by path loss and shadowing. Okumura or Hata model is one of the most extensively used models to calculate the path loss in urban areas.

2.3 Small-Scale Fading

The fading that arises when base station and mobile terminal are separated by a short distance is known as small scale fading. The small scale fading can be further divided based on the multipath effect and Doppler effect. The multipath effect occurs due to interference of signals from multiple paths. It gives the multipath profile of a channel which characterizes the frequency selectivity. The Doppler effect occurs when mobile station moves with a certain speed and the received signal varies from time to time. The delay spread and Doppler spread are the two properties that characterize the wireless channel [7].

2.3.1 Multipath Effect

The signal after passing through the channel arrives at the receiver through different paths and undergoes constructive or destructive interference. Multiple signal copies arrive over

an interval of time; this time duration is known as delay spread. The delay spread can be computed using maximum delay spread and RMS (root mean square) delay spread. The maximum delay spread is defined as the ratio of weighted delay and total power and given by:

$$\tilde{\tau} = \frac{\sum_{i=0}^{L-1} g_i \tau_i}{\sum_{i=0}^{L-1} g_i} \quad (2.2)$$

The RMS delay spread is defined as the ratio of average square deviation and total power and given by:

$$\sigma_{\tau} = \sqrt{\frac{\sum_{i=0}^{L-1} g_i (\tau_i - \tilde{\tau})^2}{\sum_{i=0}^{L-1} g_i}} \quad (2.3)$$

2.3.2 Coherence Bandwidth

The duration for which the channel frequency response remains constant is known as coherence bandwidth. If the received signal bandwidth is less than or equal to coherence bandwidth of the channel then there is no distortion in received signal. This is known as flat fading. If the received signal bandwidth is more than coherence bandwidth then there is a distortion in received signal. This is known as frequency-selective fading and this leads to inter-symbol interference (ISI). The coherence bandwidth is inversely proportional to RMS delay spread [8], which can be written as follows:

$$B_c \approx \frac{1}{\sigma_{\tau}} \Rightarrow B_c = \frac{1}{2\sigma_{\tau}} \quad (2.4)$$

2.3.3 Doppler Effect

Doppler shift is the change in frequency of electromagnetic wave arising due to relative motion between transmitter and receiver. The Doppler shift is given by:

$$f_d = \left(\frac{v \cos \theta}{c} \right) f_c \quad (2.5)$$

where C is speed of light, f_c is the carrier frequency, v is velocity of mobile terminal and θ is the angle between the BS and MS as seen in the Figure 2.2.

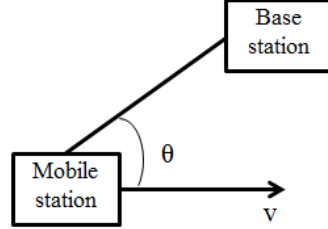


Figure 2.2: MS and BS angle representation.

2.3.4 Coherence Time

The time over which the channel properties remain constant is known as coherence time. The coherence time plays an important role in determining the time for which the channel estimation must be done. To get the knowledge of channel it has to be measured atleast once every coherent time. If the coherence time is greater than inter-channel estimation time, it is known as slow fading. If the coherence time is less than inter-channel estimation time, it is known as fast fading. Doppler spread is the spread of Doppler spectrum. The Doppler spread (B_d) is given by ' $2f_m$ ', where f_m is the maximum Doppler shift. Coherence time is inversely proportional to Doppler spread [8] and is given as:

$$T_c \approx \frac{1}{f_m} \Rightarrow T_c = \frac{1}{2B_d} \quad (2.6)$$

2.4 Doppler Spectrum

Doppler spectrum gives the intuition how fast the channel changes. It is given by [8]:

$$S_H(f) = \int_{-\infty}^{\infty} \psi(\Delta t) e^{-j2\pi f(\Delta t)} d(\Delta t) = \int_{-\infty}^{\infty} J_0(2\pi f_{dmax} \Delta t) e^{-j2\pi f_d} \quad (2.7)$$

Equation 2.7 can also be written as:

$$S_H(f) = \frac{1}{\pi f_{dmax}} \frac{\text{rect}(f/2\sin)}{\sqrt{1 - (f/f_d)^2}} \quad (2.8)$$

2.5 Rayleigh Fading

Usually the amplitude of a signal in a fading environment undergoes several scattering components. If the scattering environment follows the Rayleigh distortion, then it is said to be Rayleigh fading. The Rayleigh fading has no LOS. That means there is no stronger scattering component and no LOS between the transmitter and receiver. The most severe multipath channel is one in which no LOS path is present and channel taps are independent, which is the Rayleigh fading channel [7]. The power spectral density of the Rayleigh fading environment is given as follows:

$$f(a) = \frac{a}{\sigma^2} \exp\left\{-\frac{a^2}{2\sigma^2}\right\} \quad (2.9)$$

where 'a' is amplitude of the CIR and $2\sigma^2$ is power of NLOS component.

2.6 Ricean Fading

The fading in which LOS is present is known as Ricean fading. The fading dips are low due to fact that LOS is present along with dispersed multipaths [7]. The power spectral density of a Ricean fading environment is given as follows:

$$f(a) = \frac{a}{\sigma^2} \exp\left\{-\frac{(a^2 + A^2)}{2\sigma^2}\right\} I_0\left\{\frac{aA}{\sigma^2}\right\} \quad (2.10)$$

where 'A' is power of LOS component, the K factor is defined by $K=A^2/2\sigma^2$ and $I_0\{\}$ is Bessel function of zeroth order.

2.7 SUI Channels

SUI channels are used in real life for practical purpose of simulation. There are six types of SUI channel models and they follow Ricean fading. The power spectral density of SUI channels is given by [1]:

$$S(f) = \begin{cases} 1 - 1.72f_0^2 + 0.785f_0^4 & |f_0| \leq 1 \\ 0 & |f_0| > 1 \end{cases} \quad (2.11)$$

The six types of SUI channels have different Doppler and delay spreads, which are shown in Table 2.1. The terrain type C is defined as flat terrain with low density of trees, terrain B is defined as hilly terrain with low density of trees, and terrain A is defined as hilly terrain with heavy tree density. The SUI channels can be categorized with respect to terrain type, Doppler spread and delay spread as shown in Table 2.1.

Table 2.1 SUI channel terrain type, Doppler and delay spreads [9].

Channel	Terrain Type	Doppler Spread	Spread	LOS
SUI-1	C	Low	Low	High
SUI-2	C	Low	Low	High
SUI-3	B	Low	Low	Low
SUI-4	B	High	Moderate	Low
SUI-5	A	Low	High	Low
SUI-6	A	High	High	Low

CHAPTER 3: OFDM AND MIMO OFDM

3.1 Introduction

OFDM is a type of frequency division multiplexing (FDM) where multiple subcarriers are used instead of a single subcarrier to transmit the information data. It is a type of multicarrier modulation (MCM) in which all the subcarriers are orthogonal. Two subcarriers are said to be orthogonal if the integral of the products over the fundamental period is zero [1]. This helps in increasing the spectral efficiency as the subcarrier spacing is less compared to FDM. The overall data rate is invariant in MCM compared to single carrier modulation (SCM). If 'B' is bandwidth of a system and 'N' is number of subcarriers, then in MCM, N symbols are transmitted in N/B time period, whereas 1 symbol is transmitted every 1/B time period in SCM. Thus, the overall data rate is same.

Weinstein and Ebert, both engineers at Bell Laboratories, introduced the concept of data transmission by FDM using the discrete Fourier transform (DFT). The bank of filters in FDM were replaced with simple inverse DFT and DFT operations. The transmitter and receiver schematic along with other important steps in an OFDM block are defined in the next step.

3.1.1 Transmitter Schematic

The symbols from the bit-to-symbol modulator are converted into N parallel streams. Each stream is a subcarrier. Let $X(k)$ be the transmit symbol. Then IFFT is used to modulate the

message symbols on different subcarriers. There are N symbols on N subcarriers, which constitutes an OFDM symbol. Then the parallel-to-serial conversion of modulated symbols is done. Then cyclic prefix is added to avoid the ISI. The resultant OFDM symbol in time domain is then transmitted through the channel. The block diagram of a transmitter is shown in Figure 3.1.

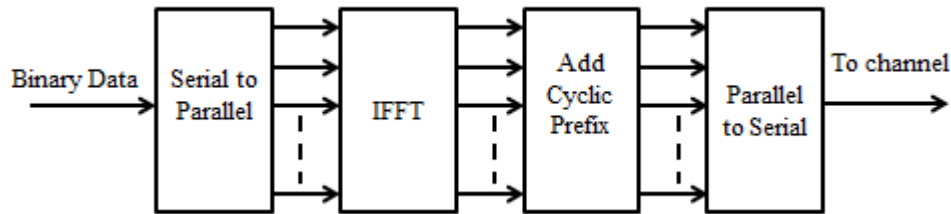


Figure 3.1: Transmitter schematic of an OFDM system.

The discrete time domain OFDM symbol $x(n)$ is given by:

$$x(n) = IDFT\{X(k)\}, \quad 0 \leq n \leq N - 1$$

$$x(n) = \sum_{k=0}^{N-1} X(k) e^{\frac{j2\pi kn}{N}} \quad (3.1)$$

3.1.2 Receiver Schematic

After the OFDM symbols pass through the frequency-selective and varying channels, they are received at the receiver. At the receiver the cyclic prefix (CP) is removed after which the signal undergoes serial-to-parallel conversion. Then they are passed through the FFT block where N -point FFT is applied to convert the signal into frequency domain and recover the transmitted symbols. The block diagram of a receiver is shown in Figure 3.2.

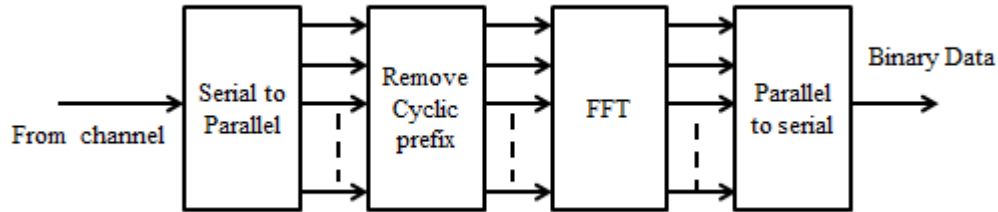


Figure 3.2: Receiver schematic of an OFDM system.

The received signal is given by:

$$Y(k) = DFT\{y(n)\}, \quad 0 \leq k \leq N - 1$$

$$Y(k) = \sum_{n=0}^{N-1} x(n) e^{-\frac{j2\pi kn}{N}} \quad (3.2)$$

$$Y(k) = X(k)H(k) + Z(k) \quad (3.3)$$

where $H(k)$ is the channel frequency response, $Z(k)$ is additive white Gaussian noise (AWGN) and the channel impulse response $h(n)$ is given by [10]:

$$h(n) = \sum_{i=0}^{L-1} h_i e^{j\frac{2\pi}{N} f_{di} \tau_n} \delta(\tau - \tau_i), \quad 0 \leq n \leq N - 1 \quad (3.4)$$

where L is the number of paths, h_i is complex CIR, f_{di} is the i^{th} path Doppler shift, τ is the delay spread index and τ_i is the i^{th} path delay.

3.1.3 Cyclic Prefix

The addition of cyclic prefix is an important stage in OFDM transmitter to prevent the ISI. The initial samples of an OFDM symbol are being subject to ISI. To avoid this we can add certain samples from the end part to the beginning of OFDM symbol. The block diagram of cyclic prefix is shown in Figure 3.3. The time-domain samples $x(0), x(1), \dots, x(N-1)$, which constitute the OFDM symbol, are transmitted from the transmitter. After passing through the

frequency-selective channel modelled by $h(0), h(1), \dots, h(L-1)$, the samples of OFDM symbol at receiver are given by [8]:

$$y(0) = h(0)x(0) + h(1)x(N-1) \dots \dots \dots + h(L-1)x(N-L+1)$$

⋮

$$y(N-1) = h(N-1)x(N-1) + h(1)x(N-1) \dots \dots \dots + h(L-1)x(N-L+1)$$

The above equation can also be written as follows:

$$[y(0) \ y(1) \ \dots \ y(N-1)] = [h(0) \ h(1) \ \dots \ h(L-1)] * [x(0) \ x(1) \ \dots \ x(L-1)]$$

$$y = h \otimes x \quad (3.5)$$

So, due to the addition of CP,

$$Y(k) = H(k)X(k) \quad (3.6)$$

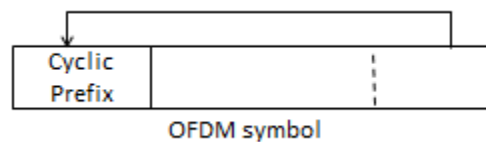


Figure 3.3: Cyclic prefix insertion.

The received symbol at k^{th} subcarrier $Y(k)$ is given by product of $H(k)$, the channel coefficient and the transmitted symbol at k^{th} subcarrier. Thus the frequency-selective channel is converted into a group of narrow flat-fading channels. The CP makes the symbol periodic and avoids ISI and inter-channel interference (ICI). OFDM converts a wideband channel into a set of N -parallel narrowband channels.

3.2 OFDM Merits

- It transforms a frequency-selective wideband channel into a number of flat-fading narrowband channels.

- The spectral efficiency of the system is increased due to orthogonal subcarriers.
- Due to addition of CP, the linear convolution converts to circular convolution, and hence avoiding ISI.
- The receiver and transmitter schematic is easier to implement compared to FDM.

3.3 OFDM Demerits

- OFDM is sensitive to timing and frequency synchronization. If the transmitter and receiver are not synchronized then it leads to ICI.
- Due to carrier frequency offset (CFO), loss of orthogonality amongst OFDM subcarriers results in ICI.
- The peak-to-average power ratio (PAPR) is high and rises with number of subcarriers. This causes saturation in the amplifier, which leads to ICI.

3.4 MIMO OFDM

To achieve high throughput, diversity and simplified reception, multiple antennas can be used both at the transmitter and receiver. MIMO OFDM is basically a combination of MIMO techniques with OFDM. Similar to OFDM, MIMO OFDM converts a frequency-selective MIMO channel into multiple parallel flat-fading MIMO channels. Hence MIMO OFDM significantly simplifies baseband receiver processing by eliminating the need for a complex MIMO equalizer.

MIMO OFDM eliminates the MIMO ISI. The total MIMO capacity is given by [8]:

$$C = \min(r, t) \left[\log_{10} \left(1 + \frac{P_t}{\sigma_n^2} \right) \right] \quad (3.7)$$

where r and t represent the number of transmit and receive antennas and P_t and σ_n^2 represent the transmitter power and noise variance. The block diagram of a MIMO system is shown in the following Figure 3.4.

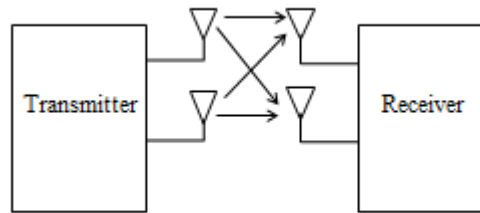


Figure 3.4: MIMO system.

The MIMO techniques are usually divided into three categories depending on the requirements like diversity, beam forming and spatial multiplexing at the receiver.

3.4.1 Spatial Diversity

With the use of multiple antennas, multiple copies of the transmitted signal are available at the receiver due to different paths which can be used to increase the diversity by improved BER. Different antennas should be separated such that there is low correlation between them. The diversity can be achieved by increasing antennas either at the transmitter or receiver. As the number of paths increases, diversity increases. The two types of diversities are transmit diversity and receiver diversity.

3.4.2 Transmit Diversity

If the number of transmit antennas is greater than 2, then transmit diversity can be performed. The CSI should be known at the transmitter to perform transmit diversity. But with the use of Alamouti space time block coding (STBC) in which coding is done in spatial and time

domains by using orthogonal codes, transmit diversity can be achieved. The Figure 3.5 shows the schematic for transmit diversity.

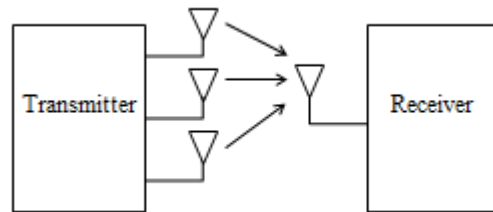


Figure 3.5: Block diagram of transmit diversity.

3.4.3 Receive Diversity

If the number of receive antennas is greater than 2, then receiver diversity can be performed. The CSI should be known at the receiver to perform receive diversity. Figure 3.6 shows the schematic for receiver diversity.

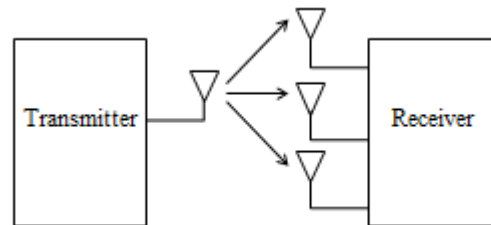


Figure 3.6: Block diagram of receive diversity.

3.4.4 Spatial Multiplexing

The MIMO system capacity can be improved by transmitting several information streams in parallel. Different data streams are transmitted from different antennas to increase the data rate by using the same bandwidth and no additional power. The antennas must be correlated to achieve spatial multiplexing. There are two types of spatial multiplexing: open-loop and closed-loop spatial multiplexing. If knowledge of channel is available and is fed back to transmitter then it is closed loop, else it is open loop multiplexing.

3.4.5 Beam Forming

It is a MIMO technique in which the overall antenna beam is targeted in the desired direction of a specific receiver antenna. The strength of the signal increases at the particular receiver antenna. It is also known as maximal ratio transmission (MRT). If antenna correlation is low, then precoding-based beam forming is used in which a precoding matrix with different complex weights is applied at the transmitter side. If the antenna correlation is high, then by applying different phase shifts to the signal at transmitter the overall beam can be directed in specific receiver direction.

3.5 Alamouti STBC

As this thesis work is related with MIMO OFDM using diversity techniques to increase the BER performance, several transmit diversity schemes introduced by Alamouti using orthogonal codes have been discussed. To perform Alamouti STBC, no CSI is necessary at the transmitter. The diversity can be increased using STBC in which the symbols are coded in spatial and time domains. Let us consider a 2x2 MIMO OFDM system, where $N_t = 2$ and $N_r = 2$ are number of transmit and receive antennas. The system can be denoted as:

$$\begin{bmatrix} Y_1(n, k) \\ Y_2(n, k) \end{bmatrix}_{2 \times 1} = \begin{bmatrix} H_{1,1}(n, k) & H_{1,2}(n, k) \\ H_{2,1}(n, k) & H_{2,2}(n, k) \end{bmatrix}_{2 \times 2} \begin{bmatrix} S_1(n, k) \\ S_2(n, k) \end{bmatrix}_{2 \times 1} + \begin{bmatrix} Z_1(n, k) \\ Z_2(n, k) \end{bmatrix}_{2 \times 1} \quad (3.8)$$

where $Y_i(n, k)$ is the received signal at n^{th} symbol and k^{th} subcarrier of i^{th} receive antenna, $H_{i,j}(n, k)$ is the channel frequency response between i^{th} receive antenna and j^{th} transmit antenna, $Z_i(n, k)$ is the AWGN at i^{th} receive antenna and $S_1(n, k)$ and $S_2(n, k)$ are transmitted symbols from transmit antennas 1 and 2, which are STBC encoded. To perform STBC, at symbol 'n' we transmit symbol $X(n, k)$ from 1st antenna and $X(n+1, k)$ from 2nd antenna. At symbol 'n+1', we

transmit $-X^*(n+1,k)$ from 1st antenna and $X^*(n,k)$ from 2nd antenna. The STBC-encoded matrix can be denoted as:

$$S = \begin{bmatrix} S_1(n,k) & S_1(n+1,k) \\ S_2(n,k) & S_2(n+1,k) \end{bmatrix} \xrightarrow{\text{Time}} \begin{bmatrix} X(n,k) & -X^*(n+1,k) \\ X(n+1,k) & X^*(n,k) \end{bmatrix} \downarrow \text{Space} \quad (3.9)$$

The received symbol at the receiver is given as follows:

At Receiver 1:

$$\begin{aligned} Y_1(n,k) &= H_{1,1}(n,k)S_1(n,k) + H_{1,2}(n,k)S_2(n,k) \\ Y_1(n+1,k) &= H_{1,1}(n+1,k)S_1(n+1,k) + H_{1,2}(n+1,k)S_2(n+1,k) \end{aligned} \quad (3.10)$$

At Receiver 2:

$$\begin{aligned} Y_2(n,k) &= H_{2,1}(n,k)S_1(n,k) + H_{2,2}(n,k)S_2(n,k) \\ Y_2(n+1,k) &= H_{2,1}(n+1,k)S_1(n+1,k) + H_{2,2}(n+1,k)S_2(n+1,k) \end{aligned} \quad (3.11)$$

Substituting the values from Equation 3.9 in the above equation, we get:

At Receiver 1:

$$\begin{aligned} Y_1(n,k) &= H_{1,1}(n,k)X(n,k) + H_{1,2}(n,k)X(n+1,k) \\ Y_1(n+1,k) &= -H_{1,1}(n+1,k)X^*(n+1,k) + H_{1,2}(n+1,k)X^*(n,k) \end{aligned} \quad (3.12)$$

At Receiver 2:

$$\begin{aligned} Y_2(n,k) &= H_{2,1}(n,k)X(n,k) + H_{2,2}(n,k)X(n+1,k) \\ Y_2(n+1,k) &= -H_{2,1}(n+1,k)X^*(n+1,k) + H_{2,2}(n+1,k)X^*(n,k) \end{aligned} \quad (3.13)$$

3.6 Alamouti SFBC

To perform Alamouti SFBC, no CSI is necessary at the transmitter. The diversity can be increased using SFBC in which the symbols are coded in spatial and frequency domains. A

detailed study of SFBC in MIMO OFDM systems has been described in [11]. Also a combination of STBC-based and SFBC-based channel estimation has been proposed in [12], but it increases complexity. Let us consider a 2x2 system, where $N_t = 2$ and $N_r = 2$ are number of transmit and receive antennas. To perform SFBC, at subcarrier 'k' of symbol n we transmit symbol $X(n,k)$ from 1st antenna and $X(n,k+1)$ from 2nd antenna. At subcarrier 'k+1', we transmit $-X^*(n,k+1)$ from 1st antenna and $X^*(n,k)$ from 2nd antenna. The SFBC-encoded matrix can be denoted as:

$$S = \begin{bmatrix} S_1(n, k) & S_1(n, k + 1) \\ S_2(n, k) & S_2(n, k + 1) \end{bmatrix} = \begin{bmatrix} X(n, k) & -X^*(n, k + 1) \\ X(n, k + 1) & X^*(n, k) \end{bmatrix} \downarrow \text{Space} \quad (3.14)$$

→ Frequency

The received symbol at the receiver is given as:

At Receiver 1:

$$\begin{aligned} Y_1(n, k) &= H_{1,1}(n, k)S_1(n, k) + H_{1,2}(n, k)S_2(n, k) \\ Y_1(n, k + 1) &= H_{1,1}(n, k + 1)S_1(n, k + 1) + H_{1,2}(n, k + 1)S_2(n, k + 1) \end{aligned} \quad (3.15)$$

At Receiver 2:

$$\begin{aligned} Y_2(n, k) &= H_{2,1}(n, k)S_1(n, k) + H_{2,2}(n, k)S_2(n, k) \\ Y_2(n, k + 1) &= H_{2,1}(n, k + 1)S_1(n, k + 1) + H_{2,2}(n, k + 1)S_2(n, k + 1) \end{aligned} \quad (3.16)$$

Substituting the values from Equation 3.14 in the above equation, we get:

At Receiver 1:

$$\begin{aligned} Y_1(n, k) &= H_{1,1}(n, k)X(n, k) + H_{1,2}(n, k)X(n, k + 1) \\ Y_1(n, k + 1) &= -H_{1,1}(n, k + 1)X^*(n, k + 1) + H_{1,2}(n, k + 1)X^*(n, k) \end{aligned} \quad (3.17)$$

At Receiver 2:

$$\begin{aligned} Y_2(n, k) &= H_{2,1}(n, k)X(n, k) + H_{2,2}(n, k)X(n, k + 1) \\ Y_2(n, k + 1) &= -H_{2,1}(n, k + 1)X^*(n, k + 1) + H_{2,2}(n, k + 1)X^*(n, k) \end{aligned} \quad (3.18)$$

3.7 Maximum Likelihood Detector

The maximum likelihood detector can be used to extract the modulated symbols from the signal received at the receiver [13]. By using the combining scheme for SFBC-encoded symbols [8], we can write the following equations:

At Receiver 1:

$$\begin{aligned} \hat{X}(n, k) &= \hat{H}^*_{1,1}(n, k)Y_1(n, k) + \hat{H}_{1,2}(n, k + 1)Y_1^*(n, k + 1) \\ \hat{X}(n, k + 1) &= \hat{H}^*_{1,2}(n, k)Y_1(n, k) - \hat{H}_{1,1}(n, k + 1)Y_1^*(n, k + 1) \end{aligned} \quad (3.19)$$

At Receiver 2:

$$\begin{aligned} \hat{X}(n, k) &= \hat{H}^*_{2,1}(n, k)Y_2(n, k) + \hat{H}_{2,2}(n, k + 1)Y_2^*(n, k + 1) \\ \hat{X}(n, k + 1) &= \hat{H}^*_{2,2}(n, k)Y_2(n, k) - \hat{H}_{2,1}(n, k + 1)Y_2^*(n, k + 1) \end{aligned} \quad (3.20)$$

The above equations can be combined as follows:

$$\begin{aligned} \hat{X}(n, k) &= \hat{H}^*_{1,1}(n, k)Y_1(n, k) + \hat{H}_{1,2}(n, k + 1)Y_1^*(n, k + 1) + \\ &\quad \hat{H}^*_{2,1}(n, k)Y_2(n, k) + \hat{H}_{2,2}(n, k + 1)Y_2^*(n, k + 1) \end{aligned} \quad (3.21)$$

$$\begin{aligned} \hat{X}(n, k + 1) &= \hat{H}^*_{1,2}(n, k)Y_1(n, k) - \hat{H}_{1,1}(n, k + 1)Y_1^*(n, k + 1) + \\ &\quad \hat{H}^*_{2,2}(n, k)Y_2(n, k) - \hat{H}_{2,1}(n, k + 1)Y_2^*(n, k + 1) \end{aligned} \quad (3.22)$$

By assuming that the channel frequency is constant for adjacent subcarriers in an OFDM symbol as shown in Equation 3.22, we can easily demodulate the SFBC-encoded data.

$$\begin{aligned} H_{i,1}[n, k] &= H_{i,1}[n, k + 1] \\ H_{i,2}[n, k] &= H_{i,2}[n, k + 1] \end{aligned} \quad (3.23)$$

Thus, the SFBC-encoded symbols can be demodulated using the above equations if we have the channel information which can be obtained using various channel estimation techniques, which are discussed in the next chapter.

CHAPTER 4: CHANNEL ESTIMATION FOR SISO AND MIMO OFDM SYSTEMS

4.1 Introduction

In a wireless communication system, the estimation of channel is necessary when the received signal is coherently demodulated. Hence, to get knowledge of the channel, it needs to be measured at least once every coherent time. The channel estimation can be done using training or pilot symbols and by blind estimation techniques [1]. The blind estimation techniques make use of statistical properties of signal to estimate the channel. But it is not applicable in fast time-varying channels as it needs a long record of data [13]. The training method uses pilot symbols which are known both at transmitter and receiver to estimate the channel. As the intensity of pilot symbols increases, the estimation accuracy increases but spectral efficiency decreases. Training method is used commonly in most of the modern communication systems as it is simple and efficient. The pilot-aided channel estimation techniques can be classified into two types.

4.2 Block-Type Pilots

The pilot symbols are inserted in frequency domain on all subcarriers in an OFDM symbol. This method of sending pilot symbols is referred to block type. The channel is assumed to be constant for a few OFDM symbols. The pilot spacing should be less than coherence time.

The block-type pilot arrangement is shown in Figure 4.1. Let S_t be the pilot spacing in time domain. Therefore S_t should satisfy the following as coherence time is inversely proportional to Doppler frequency [1].

$$S_t \leq \frac{1}{f_{doppler}} \quad (4.1)$$

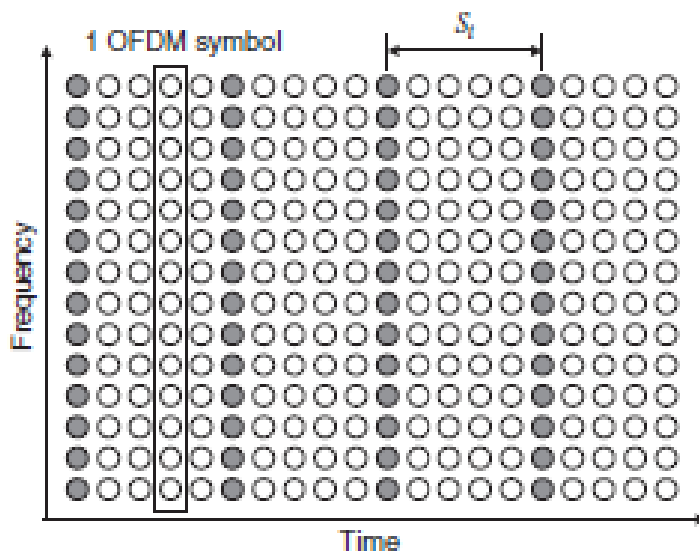


Figure 4.1: Block type pilot arrangement [1].

This type of arrangement is suitable for slow fading channel and frequency-selective channels. This type of pilot method does not work in fast time-varying channels as the channel changes from symbol to symbol.

4.3 Comb-Type Pilots

The pilot symbols are inserted in time domain at all the OFDM symbols at certain frequency spacing between the subcarriers. Thus not all the subcarriers are pilots in an OFDM symbol. The pilot spacing between pilot subcarriers should be such that it must be located as frequently as coherence bandwidth [1]. The comb type pilot arrangement is shown in Figure 4.2.

Let S_f be the pilot spacing in frequency domain. Therefore it must satisfy the following as coherence bandwidth is inversely proportional to maximum delay spread.

$$S_f \leq \frac{1}{\sigma_{maximum}} \quad (4.2)$$

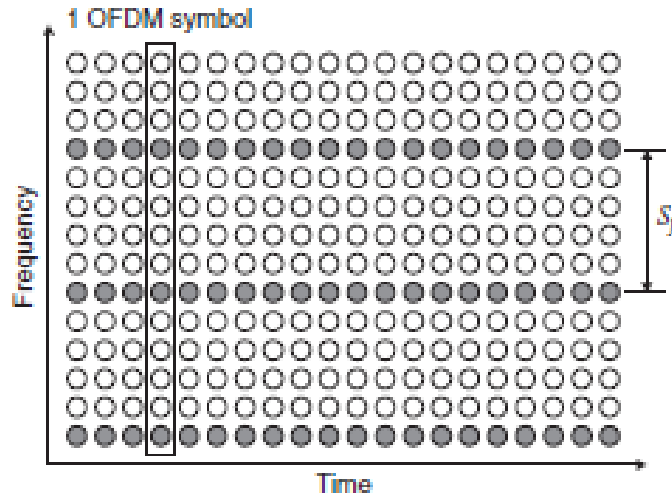


Figure 4.2: Comb type pilot arrangement [1].

This type of arrangement is able to track fast-fading channels. This type of pilot method is not applicable in frequency-selective channels. By using comb type pilots, only the frequency response at pilot subcarriers is known and the response at data subcarriers has to be determined. By using interpolation techniques, we can find the frequency response at data subcarriers.

4.3.1 Interpolation Techniques

Channel interpolation needs to be performed in comb type method to estimate the channel at data subcarriers. There are many interpolation techniques like the linear interpolation, spline interpolation, low pass interpolation, cubic spline interpolation and many more. Linear interpolation is the simplest of all techniques with moderate performance and is used in this

thesis work. In linear interpolation method, the channel estimation at data subcarriers k ($mL < k < (m+1)L$) is done using the two adjacent pilots and linearly interpolating it, given by:

$$\begin{aligned} H_e(k) &= H_e(mL + l), & 0 \leq l \leq L \\ &= \left(H_p(m+1) - H_p(m) \right) \frac{l}{L} + H_p(m) \end{aligned} \quad (4.3)$$

where $H_p(m)$ is the frequency response at pilot location.

4.4 SISO OFDM Channel Estimation

The SISO OFDM channel estimation can be performed for block type and comb type pilots by using LS and MMSE channel estimators, which are discussed in the next section. The block diagram of SISO OFDM system is shown in Figure 4.3.

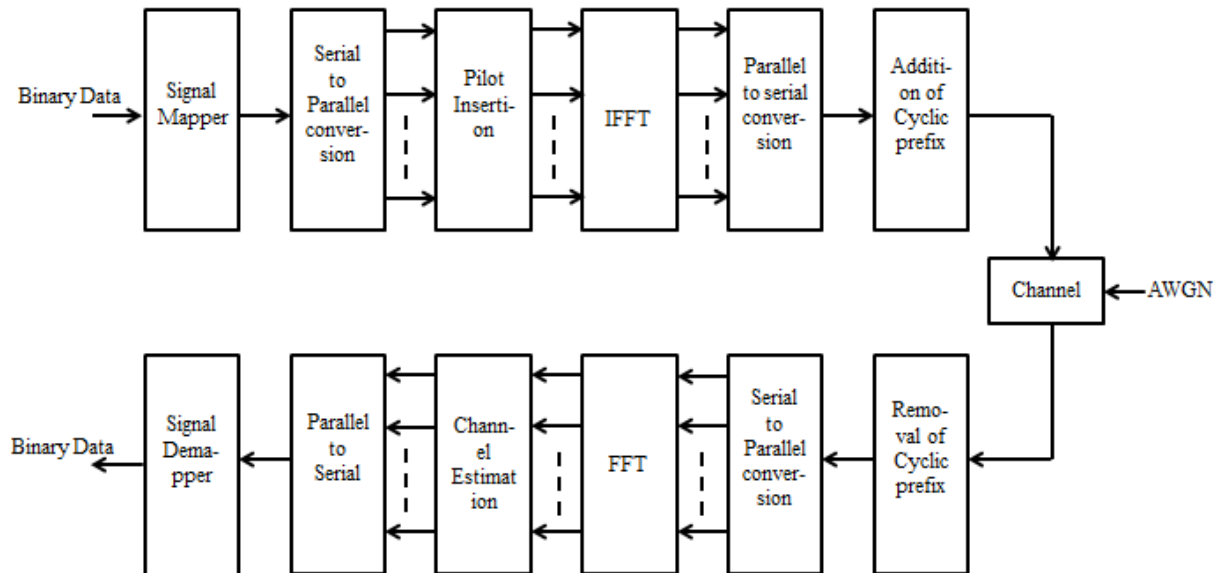


Figure 4.3: Block diagram of SISO OFDM channel estimation.

4.4.1 Using Block-Type pilots

The pilot symbols are transmitted at all the subcarriers of an OFDM symbol. If there is no ISI then we can write the received signal [13] as:

$$\begin{aligned} Y &= XH + Z \\ &= XFh + Z \end{aligned} \quad (4.4)$$

where

$$\begin{aligned} X &= \text{diag}\{X(0), X(1), \dots, X(N-1)\} \\ Y &= [Y(0), Y(1), \dots, Y(N-1)]^T \\ Z &= [Z(0), Z(1), \dots, Z(N-1)]^T \\ H &= [H(0), H(1), \dots, H(N-1)]^T \\ F &= \begin{bmatrix} W_N^{00} & \dots & W_N^{0(N-1)} \\ \vdots & \ddots & \vdots \\ W_N^{(N-1)0} & \dots & W_N^{(N-1)(N-1)} \end{bmatrix} \end{aligned} \quad (4.5)$$

where F is the NXN DFT matrix and its elements are defined as $W_N^{nk} = \frac{1}{\sqrt{N}} e^{\frac{-j2\pi nk}{N}}$.

Using Least Square Estimator:

To find the channel estimate using least square estimator we have to minimize the cost function Q [10] given by:

$$\begin{aligned} Q(\hat{H}) &= (Y - X\hat{H})^H (Y - X\hat{H}) \\ &= (Y - X\hat{H})^H (Y - X\hat{H}) \\ &= Y^H Y - Y^H X\hat{H} - \hat{H}^H X^H Y - \hat{H}^H X^H X\hat{H} \end{aligned} \quad (4.6)$$

By differentiating with respect to \hat{H} in order to minimize the above function and equating it to zero, we get:

$$\begin{aligned}\frac{\partial Q}{\partial \hat{H}} &= -2(X^H Y) + 2(X^H X \hat{H}) = 0 \\ \hat{H}_{LS} &= (X^H X)^{-1} X^H Y = X^{-1} Y\end{aligned}\quad (4.7)$$

Therefore the least square channel estimation is given by:

$$\hat{H}_{LS}(k) = \frac{Y(k)}{X(k)}, \quad k = 0, 1, \dots, N-1 \quad (4.8)$$

Using Minimum Mean Square Error Estimator:

The minimum mean square error estimator has better performance compared to least square estimator but has high complexity [14]. To find the channel estimate using minimum mean square error estimator we have to minimize the cost function Q [10], Let $\hat{H} \cong M\tilde{H}$ be the MMSE estimate where M is a weight matrix which minimizes the MSE and $\hat{H}_{LS} \cong \tilde{H} \cong X^H Y$.

$$Q(\hat{H}) = E[(H - \hat{H})^2] = E[(H - \hat{H})^H (H - \hat{H})] \quad (4.9)$$

From the orthogonality rule, the estimation error 'e' is orthogonal to \tilde{H} as shown in Figure 4.4, which is given as:

$$\begin{aligned}E\{e\tilde{H}^H\} &= E\{(H - \hat{H})\tilde{H}^H\} \\ &= E\{(H - M\tilde{H})\tilde{H}^H\} \\ &= E\{H\tilde{H}^H\} - ME\{\tilde{H}\tilde{H}^H\} \\ &= R_{H\tilde{H}} - MR_{\tilde{H}\tilde{H}} = 0\end{aligned}$$

which can be solved to give:

$$M = R_{H\tilde{H}} R_{\tilde{H}\tilde{H}}^{-1} \quad (4.10)$$

where

$$\begin{aligned}
 R_{\tilde{H}\tilde{H}} &= R_{\tilde{H}_{LS}\tilde{H}_{LS}} = E\{X^{-1}Y(X^{-1}Y)^H\} = E\{HH^H\} + E\{X^{-1}ZZ^H(X^{-1})^H\} \\
 &= R_{HH} + \frac{\sigma_Z^2}{XX^H}I = FE\{hh^H\}F^H + \frac{\sigma_Z^2}{XX^H}I_N \\
 &= XFR_{hh}F^HX^H + \sigma_Z^2I_N
 \end{aligned} \tag{4.11}$$

and

$$\begin{aligned}
 R_{H\tilde{H}} &= R_{H\tilde{H}_{LS}} = E\{Fh(Fh)^H\} \\
 &= FE\{hh^H\}F^H \\
 &= FR_{hh}F^H
 \end{aligned} \tag{4.12}$$

Therefore, the MMSE estimate is given by:

$$\begin{aligned}
 \hat{H}_{MMSE} &= R_{H\tilde{H}}R_{\tilde{H}\tilde{H}}^{-1}\tilde{H} \\
 &= FR_{hh}F^H\{XFR_{hh}F^HX^H + \sigma_Z^2I_N\}^{-1}X^HY
 \end{aligned} \tag{4.13}$$

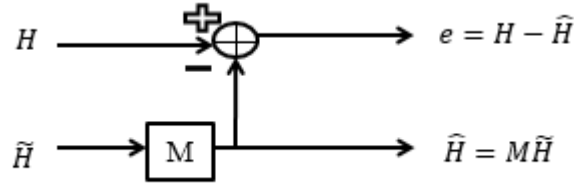


Figure 4.3: MMSE channel estimation overview.

4.4.2 Using Comb-Type pilots

The N_p pilot symbols are inserted uniformly into $X(k)$ using the formula shown below:

$$\begin{aligned}
 X(k) &= X(mL + l) \\
 &= \begin{cases} X_p(m); & l = 0 \\ \text{Information Data}; & l = 1, 2, \dots, L - 1 \end{cases}
 \end{aligned} \tag{4.14}$$

where m is pilot index. If there is no ISI then we can write the received signal as:

$$\begin{aligned}
Y_p &= X_p H_p + Z_p \\
&= X_p F_p h + Z_p
\end{aligned} \tag{4.15}$$

where $X_p = \text{diag}\{X_p(0), X_p(1), \dots, X_p(N_p - 1)\}$

$$Y_p = [Y_p(0), Y_p(1), \dots, Y_p(N_p - 1)]^T \tag{4.16}$$

Using Least Square Estimator:

The least square estimator using comb type arrangement at pilot subcarrier can be derived from Equation 4.8 as follows:

$$\hat{H}_{p,LS} = X_p^{-1} Y_p = \frac{Y_p(m)}{X_p(m)}, \quad m = 0, 1, \dots, N_p - 1 \tag{4.17}$$

Using Minimum Mean Square Error Estimator:

The MMSE estimator for comb type arrangement at pilot subcarrier can be derived from 4.13 as:

$$\hat{H}_{p,MMSE} = R_{H\hat{H}_p} R_{\hat{H}_p\hat{H}_p}^{-1} \tilde{H}_p \tag{4.18}$$

where $R_{\hat{H}_p\hat{H}_p} = R_{\hat{H}_p,LS\hat{H}_p,LS} = F R_{hh} F_p^H + \frac{\sigma_z^2}{X_p X_p^H} I_N$

and $R_{H\hat{H}_p} = R_{H\hat{H}_p,LS} = F R_{hh} F_p^H \tag{4.19}$

$$\hat{H}_{p,MMSE} = F R_{hh} F_p^H \{X_p F R_{hh} F_p^H X_p^H + \sigma_z^2 I_N\}^{-1} X_p^H Y_p \tag{4.20}$$

4.5 MIMO OFDM Channel Estimation

The MIMO OFDM channel estimation can be performed for block type and comb type pilots by using LS and MMSE channel estimators, which are discussed in the next section. The block diagram of MIMO OFDM system is shown in Figure 4.5. An optimal training pattern for least square channel estimation in MIMO OFDM systems has been proposed in [15]. In MIMO

OFDM system we use orthogonal pilots. Orthogonal pilots mean that when we transmit pilot symbol from one antenna, the other antenna remains silent or it transmits null symbol. We use SFBC-encoded MIMO OFDM system in which data and pilot symbols are SFBC encoded. Due to presence of orthogonal pilot symbols, the MIMO OFDM channel estimation is similar to SISO OFDM channel estimation. The SFBC encoded matrix for pilot estimation is given as:

$$S = \begin{bmatrix} S_1(n, k) & S_1(n, k + 1) \\ S_2(n, k) & S_2(n, k + 1) \end{bmatrix} = \begin{bmatrix} X(n, k) & 0 \\ 0 & X^*(n, k) \end{bmatrix} \downarrow \text{Space} \quad (4.21)$$

→ Frequency

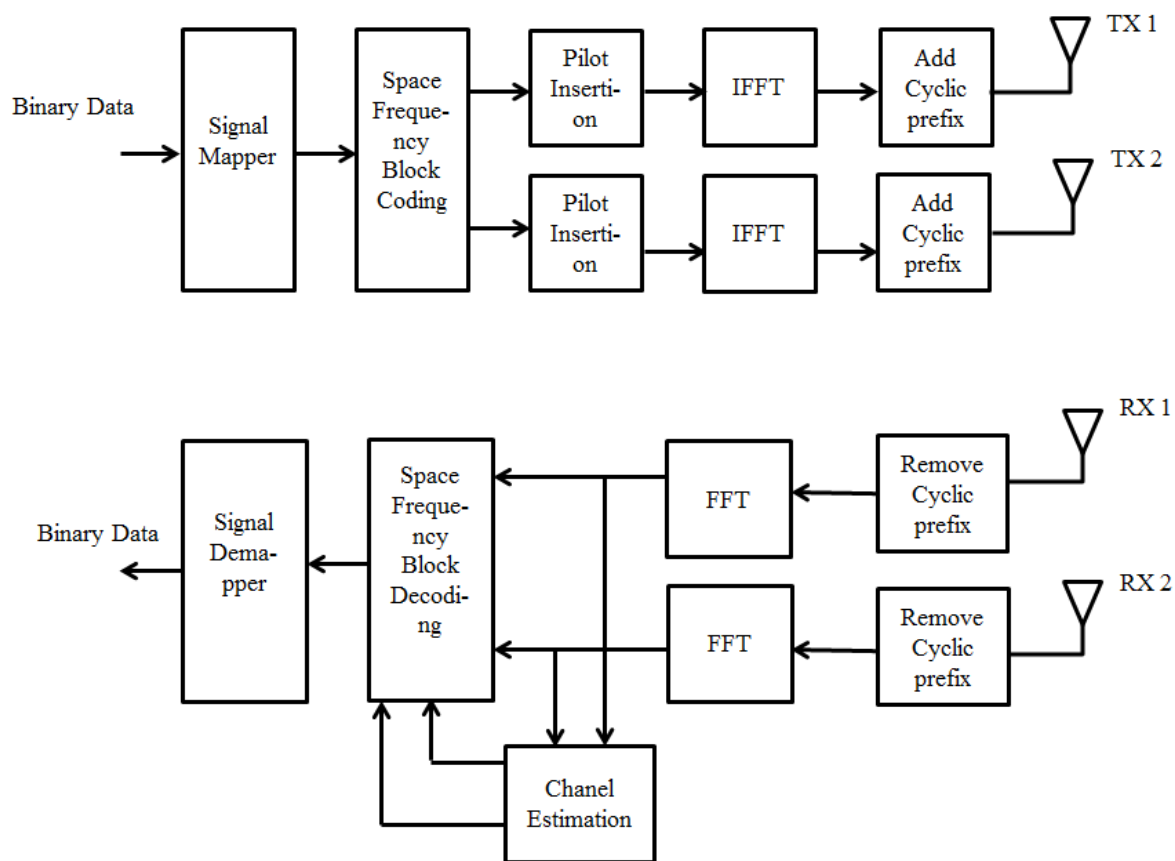


Figure 4.5: Block diagram of MIMO OFDM channel estimation.

4.5.1 Using Block-Type Pilots

Similar to SISO OFDM block type channel estimation, the LS and MMSE estimation of MIMO OFDM system is explained in the following sections.

Using Least Square Estimator:

The least square channel estimator for MIMO OFDM systems using block type pilots is given as:

$$\hat{H}_{p,LS(i,j)} = (X_j)^{-1}Y_i \quad (4.22)$$

where i, j are the transmit and receive antennas.

Using Minimum Mean Square Error Estimator:

The MMSE estimate for a MIMO OFDM system using comb type pilot symbols is given as:

$$\begin{aligned} \hat{H}_{(i,j)MMSE} &= R_{H\tilde{H}(i,j)} R_{\tilde{H}\tilde{H}(i,j)}^{-1} X_j^H Y_i \\ &= F R_{hh(i,j)} F^H \{X_j F_p R_{hh(i,j)} F_p^H X_j^H + \sigma_Z^2 I_N\}^{-1} X_j^H Y_i \end{aligned} \quad (4.23)$$

4.5.2 Using Comb-Type Pilots

The N_p pilot symbols are inserted uniformly into $X(k)$ using the formula shown below.

$$\begin{aligned} X(k) &= X(mL + l) \\ &= \begin{cases} X_p(m); & l = 0 \\ \text{Information Data}; & l = 1, 2, \dots, L - 1 \end{cases} \end{aligned} \quad (4.24)$$

where m is the pilot index.

Using Least Square Estimator:

The LS estimate for comb type arrangement in MIMO OFDM system is given as:

$$\hat{H}_{(i,j)p,LS} = X_{j_p}^{-1} Y_{i_p} \quad (4.25)$$

Using Minimum Mean Square Error Estimator:

The MMSE estimator for comb type arrangement for a MIMO OFDM system is given as:

$$\begin{aligned}\hat{H}_{(i,j)p,MMSE} &= R_{H\tilde{H}(i,j)} R_{\tilde{H}\tilde{H}(i,j)}^{-1} X_{j_p}^H Y_{i_p} \\ &= F R_{hh(i,j)} F_p^H \left\{ X_{j_p} F_p R_{hh(i,j)} F_p^H X_{j_p}^H + \sigma_z^2 I_N \right\}^{-1} X_{j_p}^H Y_{i_p}\end{aligned}\quad (4.26)$$

CHAPTER 5: SIMULATION RESULTS AND COMPARISON

The channel estimation of SISO and MIMO OFDM systems using LS and MMSE estimators with block- and comb-type pilots discussed in Chapters 4 were simulated and analyzed using MATLAB R2010a.

5.1 MSE Comparison for a Rayleigh Channel

The LS and MMSE channel estimators were simulated with block- and comb-type pilots for SISO and MIMO OFDM systems where a Rayleigh channel has been used. The channel model for a SISO OFDM system with sampling interval T_s is given by:

$$h(n) = \delta(n) + \delta(n - 0.5T_s) + \delta(n - 2.5T_s) \quad (5.1)$$

whereas the channel model for a MIMO OFDM system is given as [13]:

$$\begin{aligned} h_{11}(n) &= \delta(n) + \delta(n - 0.5T_s) + \delta(n - 3.5T_s) \\ h_{12}(n) &= \delta(n) + \delta(n - 0.3T_s) + \delta(n - 1.1T_s) \\ h_{21}(n) &= \delta(n) + \delta(n - 0.6T_s) + \delta(n - 0.9T_s) \\ h_{22}(n) &= \delta(n) + \delta(n - 0.4T_s) + \delta(n - 2.1T_s) \end{aligned} \quad (5.2)$$

The simulation parameters are mentioned in Table 5.1. The simulation is done for both SISO and MIMO OFDM systems for a bandwidth of 1 MHz in a Rayleigh fading channel. The performance evaluation of the channel estimators is done by using MSE vs SNR and BER vs SNR plots.

Table 5.1 Simulation Parameters for a Rayleigh Channel

Parameters	Specifications
FFT Size	128
No. of active subcarriers	128
Guard Interval samples	32
Bandwidth	1 MHZ
Signal Constellation	QPSK
Channel type	Rayleigh
No. of Antennas	1x1, 2x2
Pilot Type	Block, Comb
No. of symbols	64

The MSE vs SNR plot for a normalized Doppler of 0.0008 is shown in Figure 5.1. It can be observed that as the Doppler frequency is low the performance by block type pilots is better than comb type pilots. Also it can be seen that MMSE performs better than LS estimator as we assume that the channel power delay profile is known at the receiver. The MSE of SISO OFDM system is better when compared to MIMO OFDM system because we have four channels in MIMO OFDM system compared to one channel in SISO OFDM system.

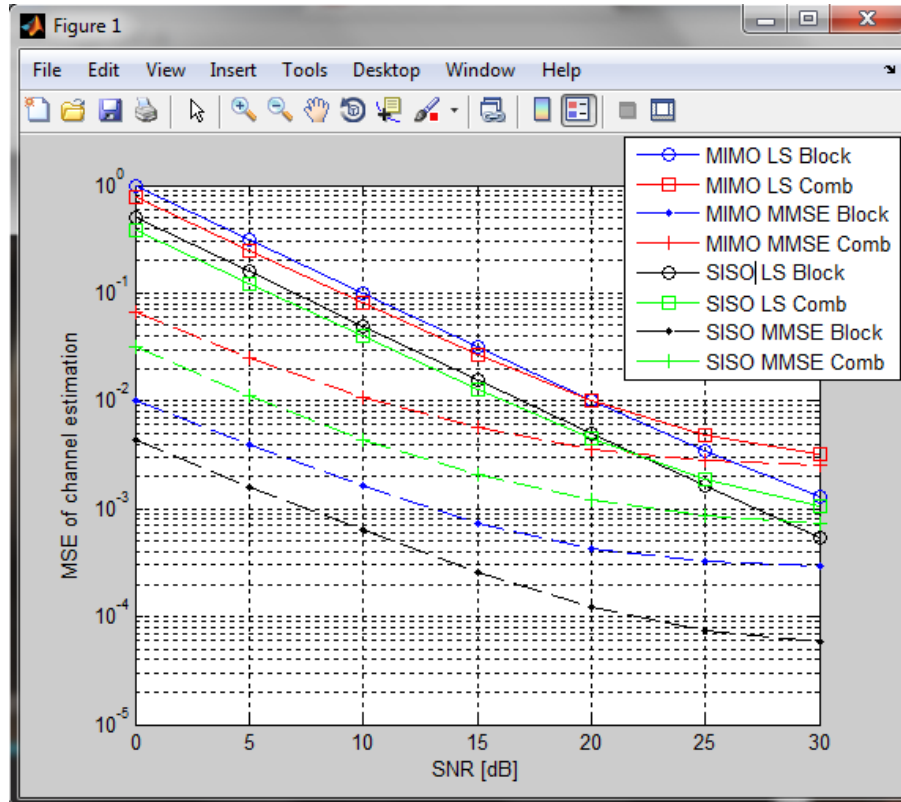


Figure 5.1 MSE vs SNR plot in a Rayleigh channel at normalized Doppler of 0.0008.

The MSE vs SNR plot for a normalized Doppler of 0.024 is shown in Figure 5.2. It can be observed that as the Doppler frequency is moderate the performance by comb type pilots is better than block type pilots. Also it can be seen that MMSE performs better than LS estimator as we assume that the channel power delay profile is known at the receiver. The MSE of SISO OFDM system is better when compared to MIMO OFDM system.

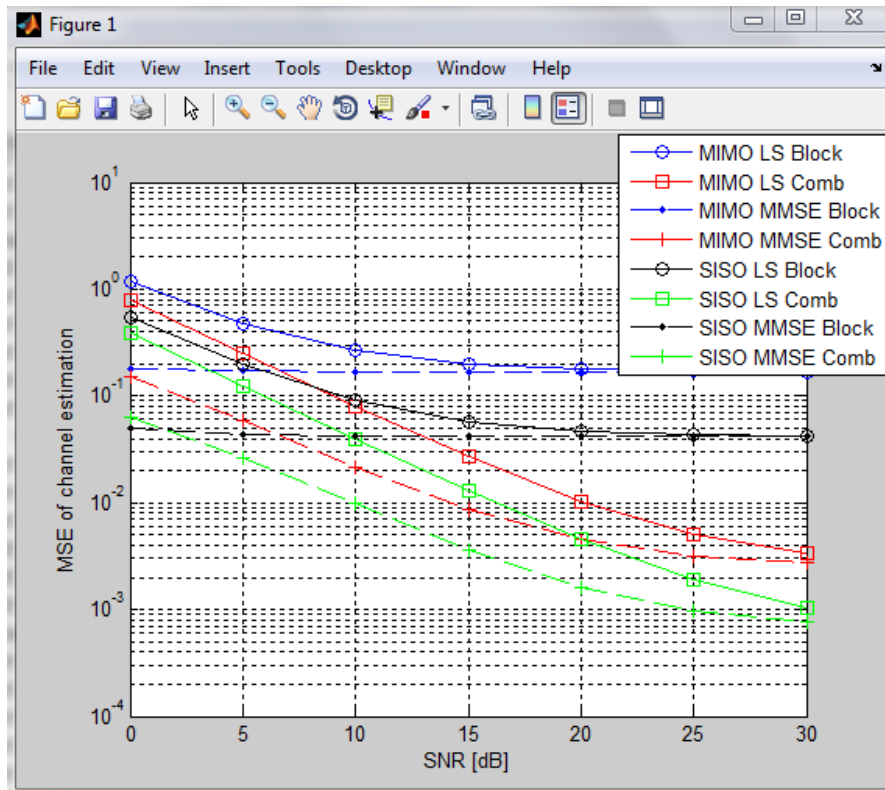


Figure 5.2 MSE vs SNR plot in a Rayleigh channel at normalized Doppler of 0.024.

The MSE vs SNR plot for a normalized Doppler of 0.048 is shown in Figure 5.3. It can be observed that as the Doppler frequency is high the performance by comb type pilots is better than block type pilots. Also it can be seen that MMSE performs better than LS estimator as we assume that the channel power delay profile is known at the receiver. The MSE of SISO OFDM system is better when compared to MIMO OFDM system.

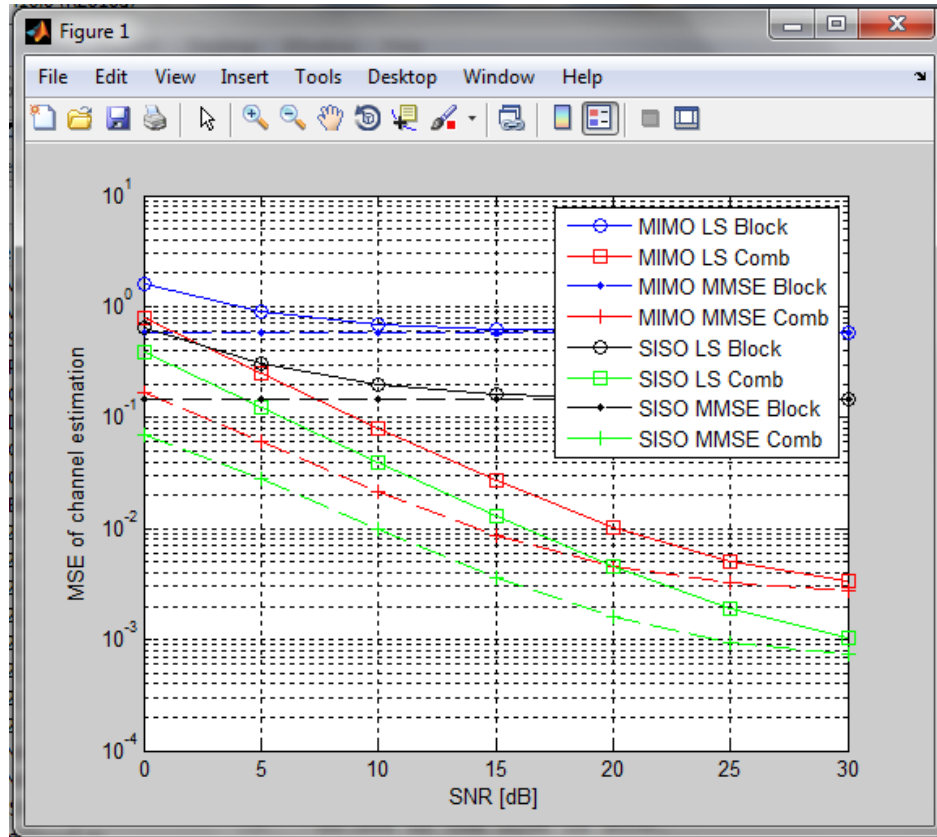


Figure 5.3 MSE vs SNR plot in a Rayleigh channel at normalized Doppler of 0.048.

5.2 BER Comparison for a Rayleigh Channel

The BER vs SNR plot for a normalized Doppler of 0.0008 is shown in Figure 5.4. It can be observed that as the Doppler frequency is low the performance by block type pilots is better than comb type pilots. Also it can be seen that MMSE performs better than LS estimator as we assume that the channel power delay profile is known at the receiver. The BER of MIMO OFDM system is better when compared to SISO OFDM system due to the fact that by increasing the number of antennas and using SFBC the diversity increases.

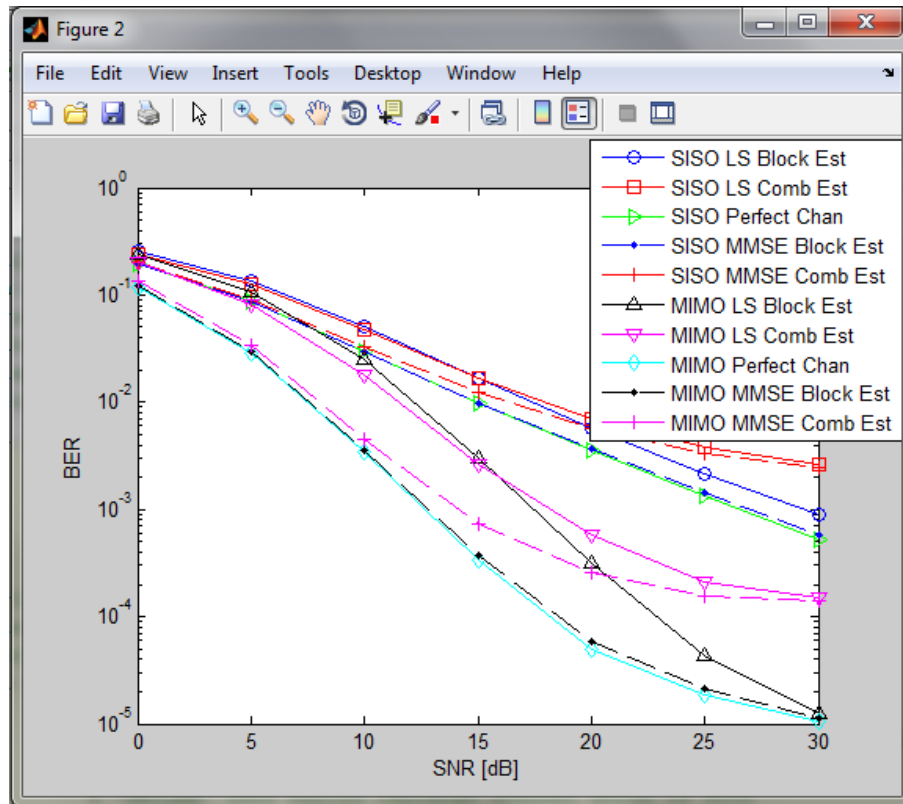


Figure 5.4 BER vs SNR plot in a Rayleigh channel at normalized Doppler of 0.0008.

The BER vs SNR plot for a normalized Doppler of 0.024 is shown in Figure 5.5. It can be observed that as the Doppler frequency is moderate the performance by comb type pilots is better than block type pilots. Also it can be seen that MMSE performs better than LS estimator as we assume that the channel power delay profile is known at the receiver. The BER of MIMO OFDM system is better when compared to SISO OFDM system.

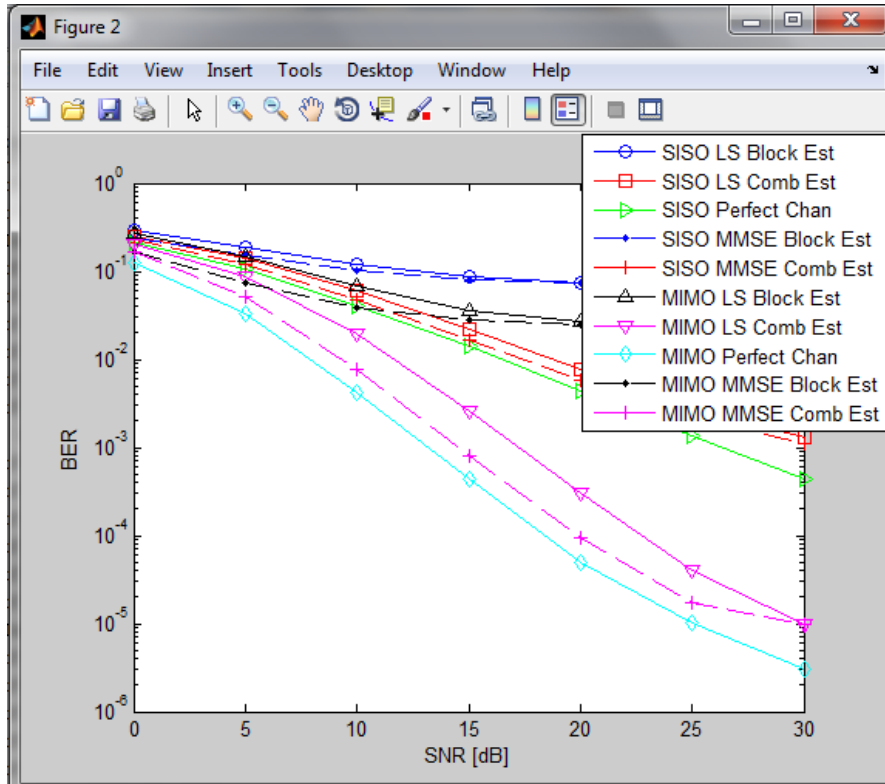


Figure 5.5 BER vs SNR plot in a Rayleigh channel at normalized Doppler of 0.024.

The BER vs SNR plot for a normalized Doppler of 0.048 is shown in Figure 5.6. It can be observed that as the Doppler frequency is high the performance by comb type pilots is better than block type pilots. Also it can be seen that MMSE performs better than LS estimator as we assume that the channel power delay profile is known at the receiver. The BER of MIMO OFDM system is better when compared to SISO OFDM system.

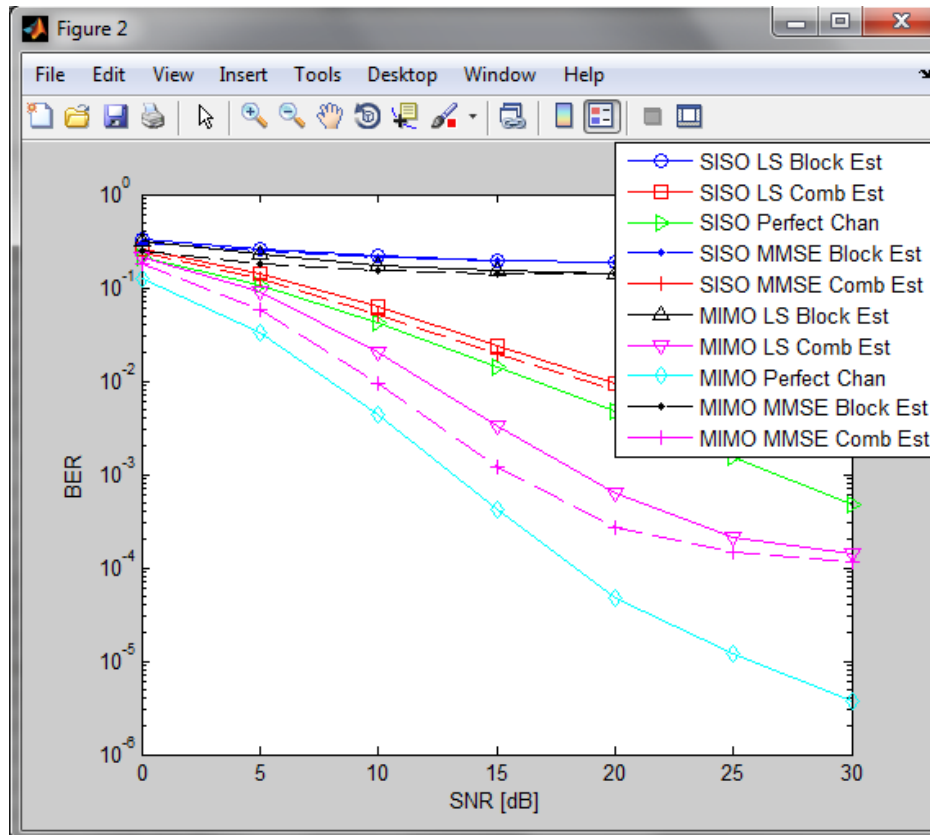


Figure 5.6 BER vs SNR plot in a Rayleigh channel at normalized Doppler of 0.048.

5.3 MSE Comparison for a SUI-3 Channel

The LS and MMSE channel estimators were simulated with block- and comb-type pilots for SISO and MIMO OFDM systems where an SUI-3 channel has been used. The parameters of SUI-3 channel are defined in the Table 5.2.

Table 5.2 SUI-3 Channel Parameters

Tap	Delay(μ s)	Gain(db)
1	0	0
2	0.4	-5
3	0.9	-10

SUI channel models have LOS component. The simulation parameters are mentioned in Table 5.3. The simulation is done for both SISO and MIMO OFDM systems for a bandwidth of 1 MHz in a Rayleigh fading channel. The performance evaluation of the channel estimators is done by using MSE vs SNR and BER vs SNR plots.

Table 5.3 Simulation Parameters for a SUI-3 Channel

Parameters	Specifications
FFT Size	128
No. of active subcarriers	128
Guard Interval samples	32
Bandwidth	1 MHz
Signal Constellation	QPSK
Channel type	SUI-3
No. of Antennas	1x1, 2x2
Pilot Type	Block, Comb
No. of symbols	64

The MSE vs SNR plot for a normalized Doppler of 0.0008 is shown in Figure 5.7. It can be observed that as the Doppler frequency is low the performance by block type pilots is better than comb type pilots. Also it can be seen that MMSE performs better than LS estimator as we assume that the channel power delay profile is known at the receiver. The MSE of SISO OFDM system is better when compared to MIMO OFDM. The performance is better in SUI-3 channel

when compared with Rayleigh channel due to the presence of LOS component in SUI channel models.

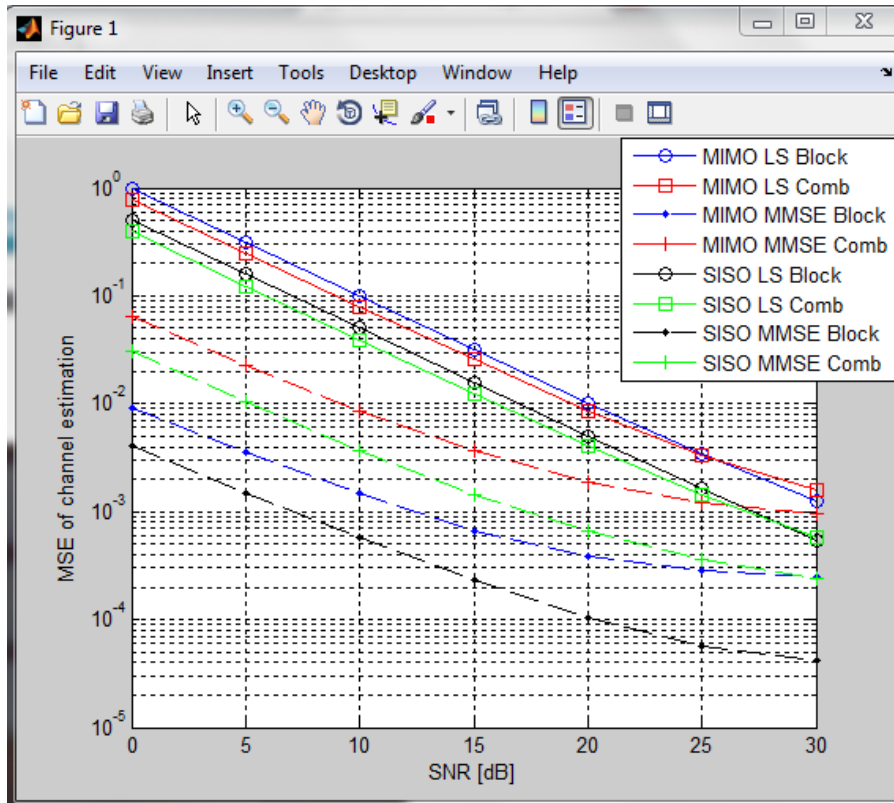


Figure 5.7 MSE vs SNR plot in a SUI-3 channel at normalized Doppler of 0.0008.

The MSE vs SNR plot for a normalized Doppler of 0.024 is shown in Figure 5.8. It can be observed that as the Doppler frequency is moderate the performance by comb type pilots is better than block type pilots. Also it can be seen that MMSE performs better than LS estimator as we assume that the channel power delay profile is known at the receiver. The MSE of SISO OFDM system is better when compared to MIMO OFDM system.

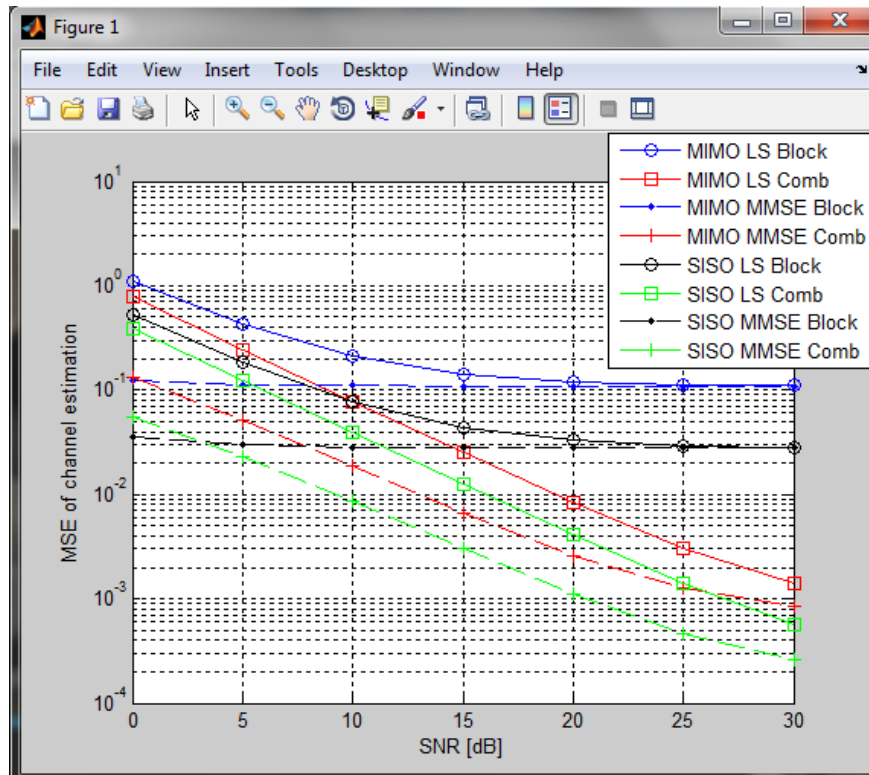


Figure 5.8 MSE vs SNR plot in a SUI-3 channel at normalized Doppler of 0.024.

The MSE vs SNR plot for a normalized Doppler of 0.048 is shown in Figure 5.9. It can be observed that as the Doppler frequency is high the performance by comb type pilots is better than block type pilots. Also it can be seen that MMSE performs better than LS estimator as we assume that the channel power delay profile is known at the receiver. The MSE of SISO OFDM system is better when compared to MIMO OFDM system.

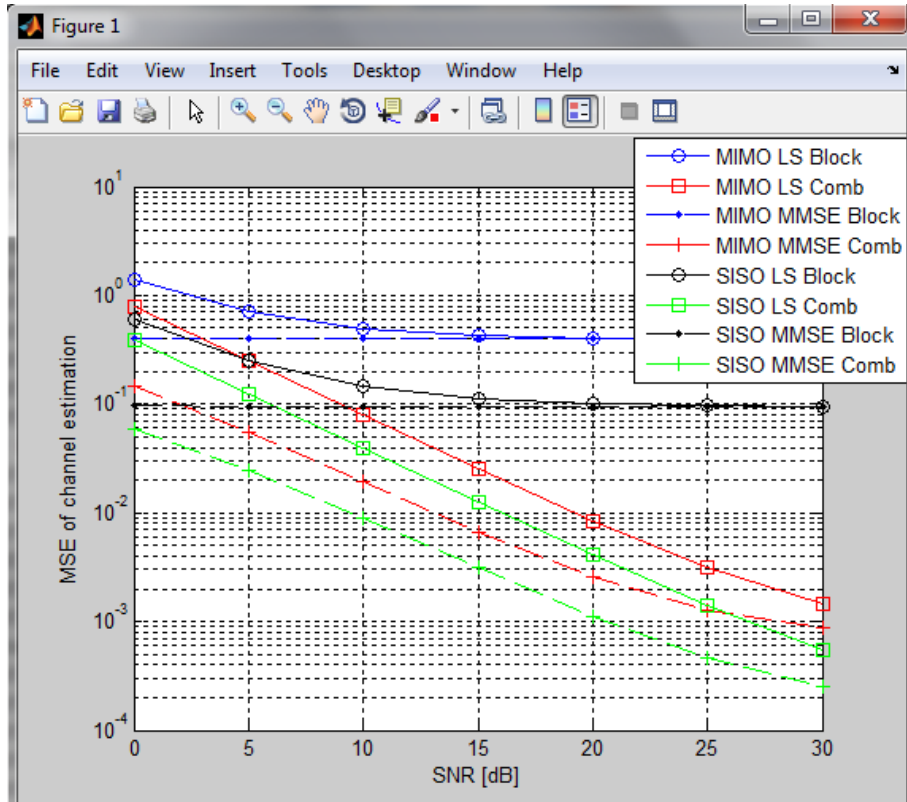


Figure 5.9 MSE vs SNR plot in a SUI-3 channel at normalized Doppler of 0.048.

5.4 BER Comparison for a SUI-3 Channel

The BER vs SNR plot for a normalized Doppler of 0.0008 is shown in figure 5.10. It can be observed that as the Doppler frequency is low the performance by block type pilots is better than comb type pilots. Also it can be seen that MMSE performs better than LS estimator as we assume that the channel power delay profile is known at the receiver. The BER of MIMO OFDM system is better when compared to SISO OFDM system due to the fact that by increasing the number of antennas and using SFBC the diversity increases. Also the performance of SUI channel model is better than Rayleigh channel due to the presence of LOS component.

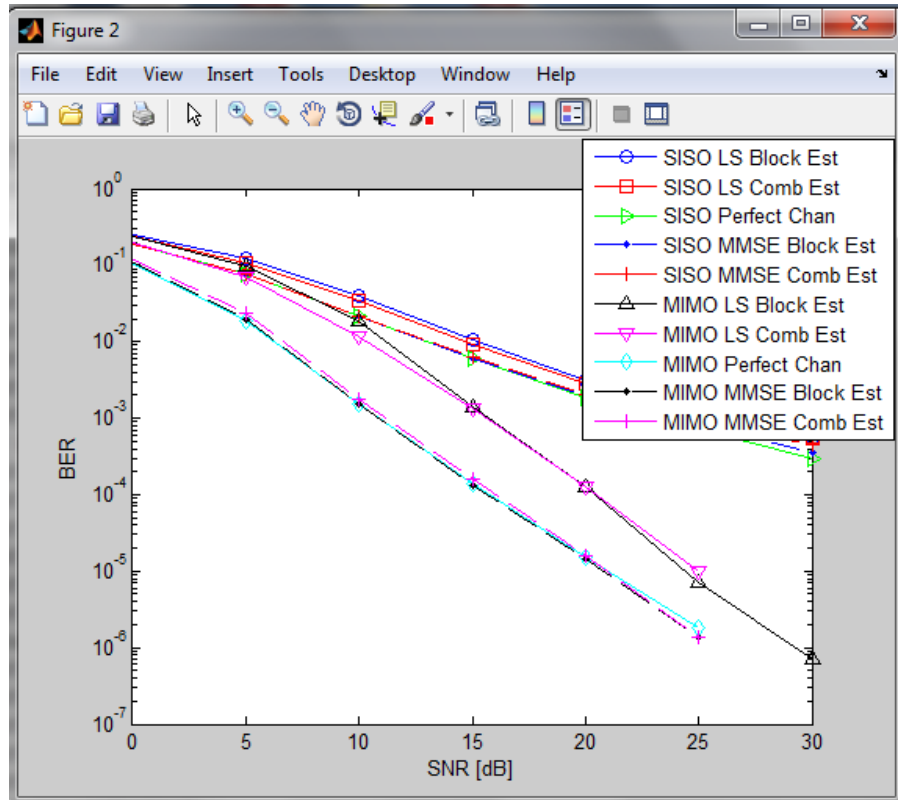


Figure 5.10 BER vs SNR plot in a SUI-3 channel at normalized Doppler of 0.0008.

The BER vs SNR plot for a normalized Doppler of 0.024 is shown in Figure 5.11. It can be observed that as the Doppler frequency is moderate the performance by comb type pilots is better than block type pilots. Also it can be seen that MMSE performs better than LS estimator as we assume that the channel power delay profile is known at the receiver. The BER of MIMO OFDM system is better when compared to SISO OFDM system.

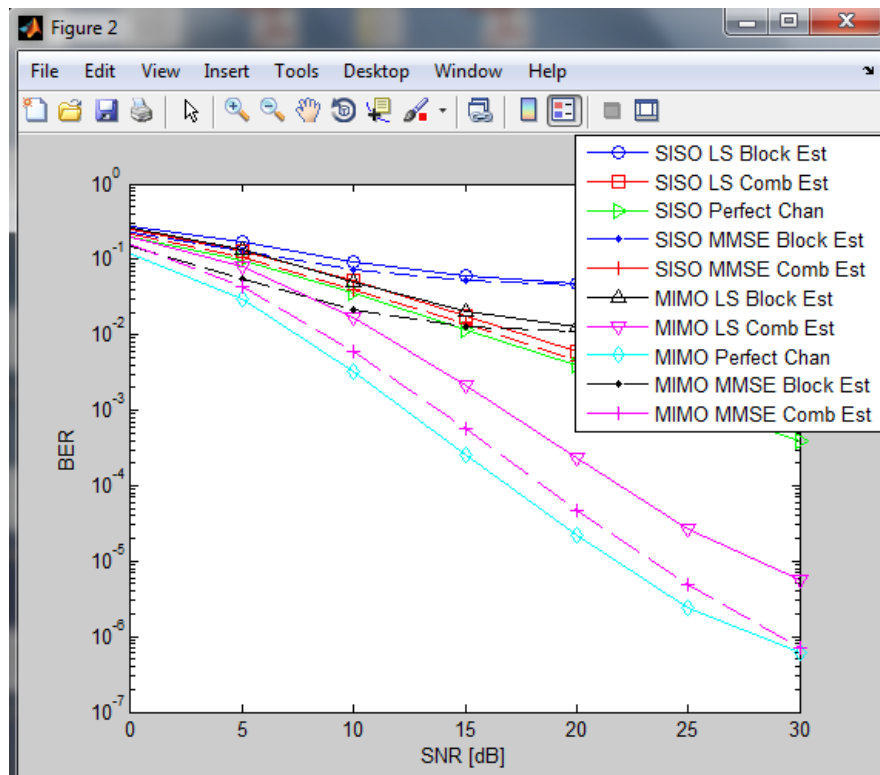


Figure 5.11 BER vs SNR plot in a SUI-3 channel at normalized Doppler of 0.024.

The BER vs SNR plot for a normalized Doppler of 0.048 is shown in Figure 5.12. It can be observed that as the Doppler frequency is high the performance by comb type pilots is better than block type pilots. Also it can be seen that MMSE performs better than LS estimator as we assume that the channel power delay profile is known at the receiver. The BER of MIMO OFDM system is better when compared to SISO OFDM system.

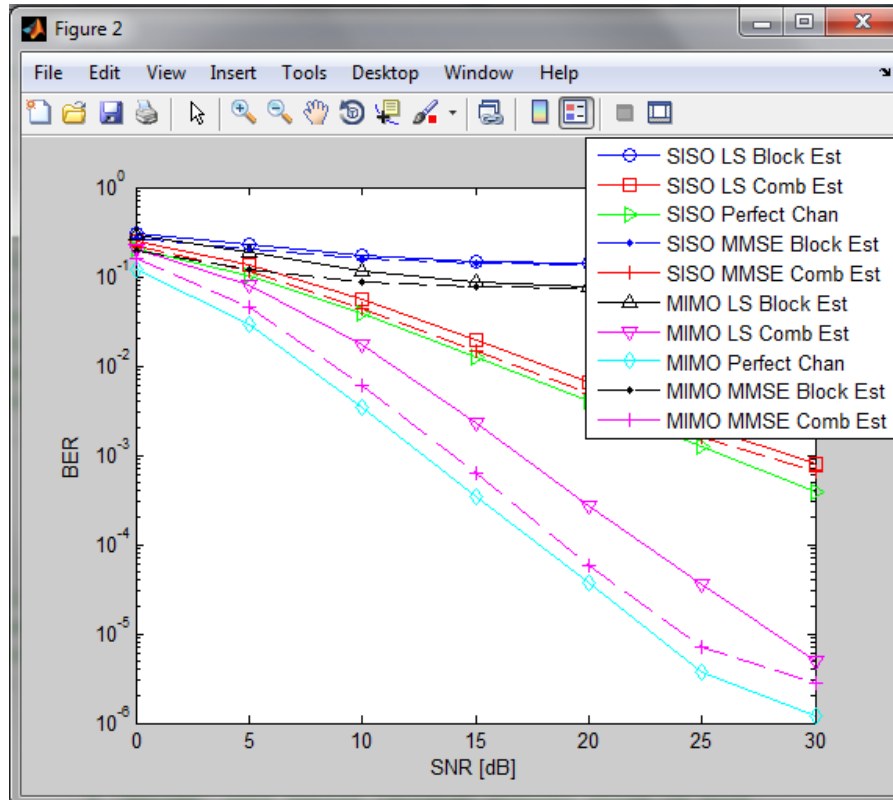


Figure 5.12 BER vs SNR plot in a SUI-3 channel at normalized Doppler of 0.048.

5.5 BER vs Normalized Doppler Comparison for a Rayleigh Channel

The BER vs normalized Doppler plot is shown in Figure 5.13. It can be observed that as the normalized Doppler increases, BER increases due to the fact that with increase in Doppler frequency the channel becomes fast time varying and it becomes difficult to estimate the channel before it changes.

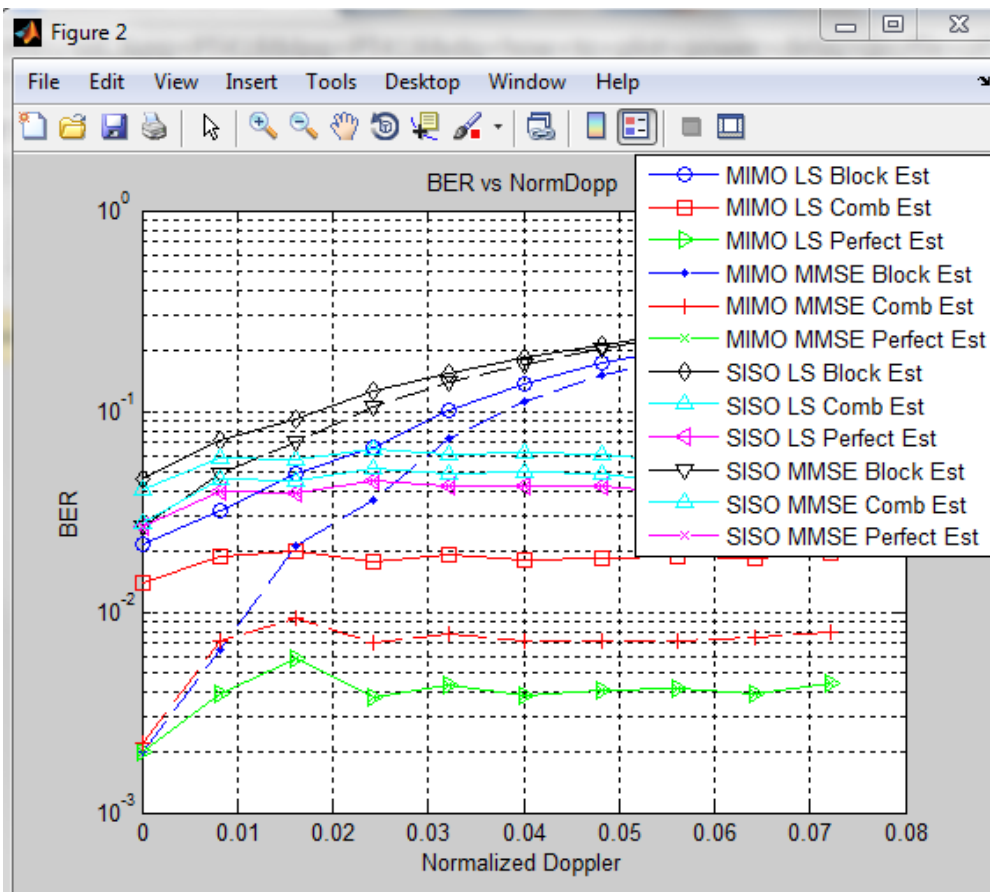


Figure 5.13 BER vs normalized Doppler plot for Rayleigh channel at SNR=12db.

5.6 BER vs Normalized Doppler Comparison for a SUI-3 channel

The BER vs normalized Doppler plot is shown in Figure 5.14. It can be observed that as the normalized Doppler increases, BER increases due to the fact that with increase in Doppler frequency the channel becomes fast time varying and it becomes difficult to estimate the channel before it changes. Also, the SUI-3 channel performance is better than Rayleigh channel.

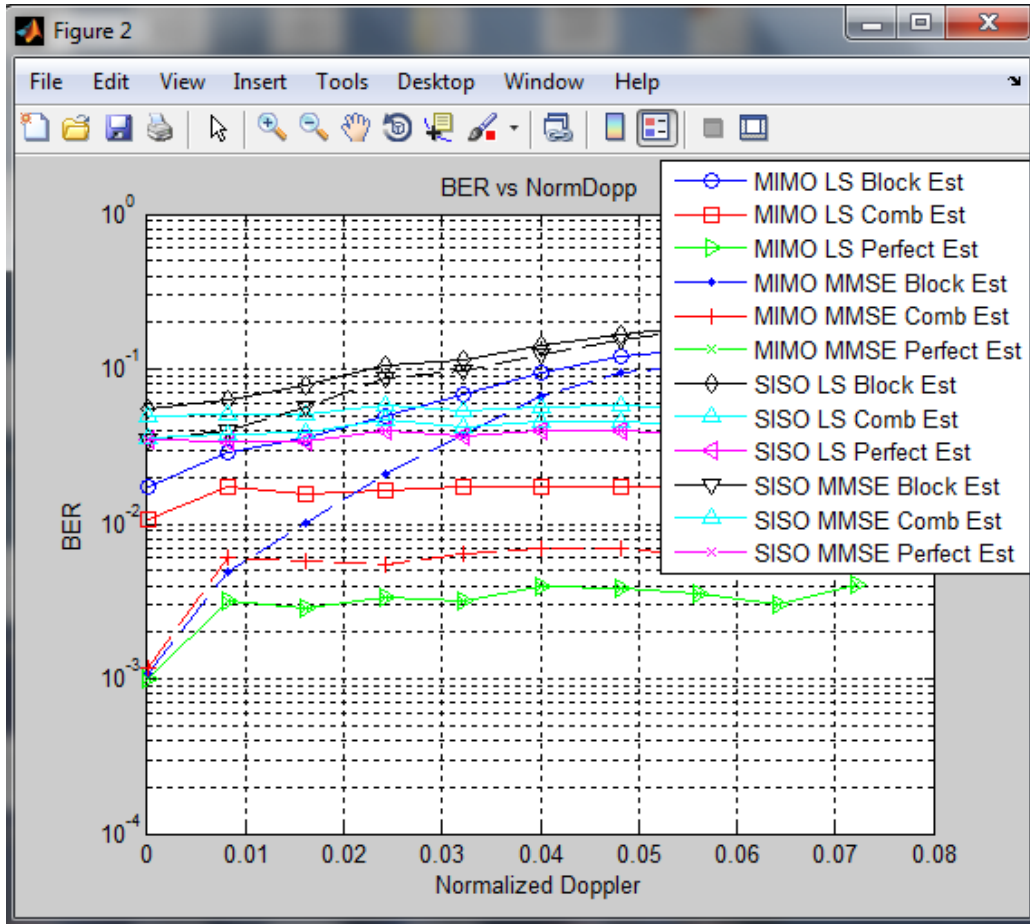


Figure 5.14 BER vs normalized Doppler plot for SUI-3 channel at SNR=12db.

CHAPTER 6: CONCLUSION AND FUTURE WORK

6.1 Conclusion

The channel estimation of SISO and MIMO OFDM systems using LS and MMSE channel estimators for block type and comb type pilots have been simulated at different Doppler frequencies and different channel scenarios like the Rayleigh fading and SUI-3 channel model. The performance of the channel estimators is evaluated using the MSE and BER plots.

The MMSE channel estimator performs better than LS estimator but it involves a matrix inversion. So, the improvement in performance comes with some complexity and also the receiver has to know CSI to perform MMSE estimation.

The MSE vs SNR and BER vs SNR plots of both SISO and MIMO OFDM systems have been plotted. The BER performance of MIMO OFDM systems is better compared to SISO OFDM systems as the diversity of MIMO OFDM systems is increased by using SFBC scheme. Also, the performance in SUI-3 channel environment is better compared to Rayleigh channel environment due to the presence of LOS component in SUI-3 channel model.

At low Doppler frequencies MMSE estimator using block type pilots performs better while at high Doppler frequencies MMSE estimator using comb type pilots performs better. Hence, the comb type MMSE estimator in MIMO OFDM is optimal in fast-fading scenarios.

6.2 Future Work

The future work may include channel estimation using a combination of block type and comb type pilots. Also, ICI is not considered in this thesis work. So, channel estimation techniques considering ICI can also be developed. As SFBC is used in this work, channel estimation schemes for a combination of spatial multiplexing and spatial diversity systems may be developed.

REFERENCES

- [1] Y. S. Cho, J. Kim, W. Y. Yang and C. Kang, *MIMO-OFDM Wireless Communications with MATLAB*, John Wiley & Sons (Asia) Pte Ltd, Singapore, 2010.
- [2] L. Wang and B. Jezek. "OFDM Modulations Schemes for Military Satellite Communications," presented at Mil. Commun. Conf., San Diego, USA, 2008.
- [3] T. Hwang, C. Yang, G. Wu, S. Li and G. Y. Li, "OFDM and Its Wireless Applications: A Survey," *IEEE Trans.*, vol. 58, no.4, May 2009.
- [4] Y. G. Li, "Simplified Channel Estimation for OFDM Systems with Multiple Transmit Antennas," *IEEE Transactions on Wireless Communications*, vol. 1, no. 1, pp. 67–75, 2002.
- [5] Wang Liping, "Channel Estimation and Combining Orthogonal Pilot Design in MIMO-OFDM System," *Journal of Networks*, vol. 9, no. 2, February 2014.
- [6] Tanairat Mata, Katsuhiro Naito, Pisit Boonsrimuang, Kazuo Mori and Hideo Kobayashi, "Proposal of Channel Estimation Method for ITS systems by using STBC MIMO-OFDM," *ECTI Transactions on Computer and Information Technology*, vol.8, no.1, May 2014.
- [7] Asad Mehmood and Waqas Aslam Cheema, "Channel Estimation for LTE Downlink," Master's Thesis, Blekinge Institute of Technology, September 2009.

- [8] A. K. Jagannatham, Online Lecture, “Advanced 3G and 4G Wireless Mobile Communications,” Faculty of Electrical Engineering, Indian Institute of Technology, Kanpur, Uttar Pradesh, retrieved online.
- [9] http://www.cse.wustl.edu/~jain/cse574-08/ftp/channel_model_tutorial.pdf
- [10] A. K. Pattanayak, “Channel Estimation in OFDM Systems,” Master’s Thesis, National Institute of Technology, Rourkela, 2007.
- [11] R. R. Kumar, “Study of SFBC MIMO OFDM in Rayleigh Fading Channel,” Master’s Thesis, Indian Institute of Technology, Roorkee, 2012.
- [12] Fabien Delestre, “Channel Estimation and Performance Analysis of MIMO-OFDM Communications using Space-Time and Space-Frequency Coding Schemes,” Ph. D Thesis, University of Hertfordshire, United Kingdom, June 2011.
- [13] K. P. Bagadi and Prof. Susmita Das, “MIMO-OFDM Channel Estimation using Pilot Carries,” *International Journal of Computer Applications* (0975 – 8887) Volume 2, No.3, May 2010.
- [14] J. J. Van de Beek, O. Edfors, M. Sandell, S. K. Wilson, and P. O. Borjesson, “On Channel Estimation in OFDM Systems,” in Proc. IEEE 45th Vehicular Technology Conf., Chicago, IL, Jul. 1995, pp. 815–819.
- [15] I. Barhumi, G. Leus and M. Moonen, “Optimal Training Design for MIMO OFDM Systems in Mobile Wireless Channels,” *IEEE transactions on signal processing*, Vol. 51, No. 6, June 2003.